

An improved flexible representation of quantum images



By

Rabia Amin Khan

2015-NUST-MS-IS-118746

Supervisor

Dr. Shahzad Saleem

Department of Computing

A thesis submitted in partial fulfillment of the requirements for the degree
of Masters of Science in Information Security (MSIS)

In

School of Electrical Engineering and Computer Science,
National University of Sciences and Technology (NUST),
Islamabad, Pakistan.

(May 2019)

Approval

It is certified that the contents and form of the thesis entitled “**An improved flexible representation of quantum images**” submitted by Rabia Amin Khan have been found satisfactory for the requirement of the degree.

Advisor: **Dr. Shahzad Saleem**

Signature: _____

Date: _____

Committee Member 1: **Dr. Asad Waqar Malik**

Signature: _____

Date: _____

Committee Member 2: **Dr Jhanzaib Shahid**

Signature: _____

Date: _____

Committee Member 3: **Dr. Syed Taha Ali**

Signature: _____

Date: _____

Dedication

I dedicate this thesis to my beloved parents and family for their tremendous cooperation and support that led this research to wonderful accomplishment.

Certificate of Originality

I hereby declare that this submission is my own work and to the best of my knowledge it contains no materials previously published or written by another person, nor material which to a substantial extent has been accepted for the award of any degree or diploma at NUST SEECS or at any other educational institute, except where due acknowledgement has been made in the thesis. Any contribution made to the research by others, with whom I have worked at NUST SEECS or elsewhere, is explicitly acknowledged in the thesis.

I also declare that the intellectual content of this thesis is the product of my own work, except for the assistance from others in the project's design and conception or in style, presentation and linguistics which has been acknowledged.

Author Name: Rabia Amin Khan

Signature: _____

Acknowledgment

I would like to express my sincere gratitude to my research supervisor Dr Shahzad Saleem for providing excellent guidance, assistance and encouragement during my MS research. His constant support was fundamental to the process of this research work. I would like to thank all my GEC members for their valuable suggestion and cooperation. And I am very thankful to my parents and my family for their moral support, encouragement and prayers.

Table of Contents

1	Introduction	2
1.1	Background and motivation	2
1.2	Brief overview of prior state of art	3
1.3	Limitations of existing models	3
1.4	Problem statement and proposed solution	4
1.5	Contributions	4
1.6	Organization of thesis	5
2	Background knowledge	7
2.1	Basic mathematical knowledge	7
2.2	Strength of quantum computer	14
2.2.1	Entanglement	14
2.2.2	Quantum mechanics's postulates	14
3	Literature Review	15
3.1	QIR models for color images	15
3.1.1	The MCQI Representation	16
3.1.2	The QMCR model	16
3.1.3	The NCQI representation	16
3.1.4	The QRCI representation	16
3.2	QIR models for grey-scale images	17
3.2.1	Qubit lattice	17
3.2.2	Real ket	17
3.2.3	Entangled image	18
3.2.4	FRQI	18
3.2.5	NEQR	19
4	Methodology	20
4.1	Analysis of FRQI	20
4.2	An improved flexible representation of quantum images	23
4.2.1	Quantum image preparation	24

TABLE OF CONTENTS

vi

4.2.2	IFRQI storage and its retrieval	27
4.2.3	Image processing operations	29
4.2.4	IFRQI compression	32
5	Discussion, Conclusion and Future Directions	39
5.1	Discussion and conclusion	39
5.2	Contributions	40
5.3	Future research directions	40

List of Abbreviations

QIQC: Quantum information and quantum computation

QIP : Quantum image processing

QIR: Quantum image representations

FRQI: A flexible representation of quantum images

NEQR: A novel enhanced quantum representation for digital images

IFRQI: Improved flexible representation of quantum images

MCQI: Multi-channel representation for quantum images

QMCR: Red-Green-Blue multi channel representation of digital images

NCQI: A novel quantum representation of color digital images

QRCI: A new quantum representation model of color images

H : Hadamard gate

I : Identity gate

X : Not gate

U : Unitary

W : Special unitary

List of Tables

2.1	Properties of complex numbers	8
4.1	Proposed method for encoding 2-bit information	24
4.2	Quantum states for the proposed encoding scheme and their probability distributions	29
4.3	Reduced quantum operations for the four groups of Figure 4.2.4	36

List of Figures

1.1	Quantum information and quantum computation	3
2.1	Basis quantum gate, their circuit diagrams and matrix representations	13
3.1	An example image with its FRQI state	18
3.2	A 2×2 image and its NEQR state	19
4.1	Controlled rotation gate $C^1(R_y(2\theta))$	21
4.2	The decomposed quantum circuit for $C^5(U)$; q_0 to q_5 are operating qubits, while a_1 to a_3 are supporting qubits	22
4.3	The ordering of pixels positions of a 4×4 image	24
4.4	Quantum image preparation process of IFRQI model	24
4.5	(a) Quantum circuit for \overline{G}_1 ; (b) Quantum circuit for \overline{G}_2 ; (c) Quantum circuit for \overline{G}_3	30
4.6	Flow chart of the IFRQI compression procedure	34
4.7	(a) an example of 8×8 image; (b) the gray-scale color value of pixel at each position; (c) p groups of quantum operation	35
4.8	Example images with gray-scale distributions	37
4.9	Comparison of number of gates used in quantum circuits of different image representation models	38

Abstract

Quantum image representations are the models that are used to represent digital images on to the quantum computers. They also allow to perform various image processing operations on these images and to store on to the quantum system. For storing images on to the quantum computers, QIR models use qubits. The FRQI and NEQR are well-known models used for capturing and processing quantum images. But these models have some weaknesses especially they suffer from time and space complexity respectively. Therefore, in this research, we establish that the complexity of image preparation in FRQI model is $O(n2^{2n})$, which is linear in the size of image. Moreover, by analyzing the FRQI and NEQR models, we propose an improved flexible representation of quantum images (IFRQI) which takes p qubits to encode gray-scale values of pixels of a $2p$ -bit-deep image. The gray-scale values are encoded by employing rotation matrices corresponding to chosen values of angles which assist in accurate retrieval of original image information through projective measurements. The quantum image compression algorithm and basic image processing operations are discussed in detail to establish the effectiveness of IFRQI model. The performance analysis in respect of time and space complexity exhibits that the IFRQI model is comparable to FRQI and NEQR models.

Chapter 1

Introduction

1.1 Background and motivation

Quantum computation is an exciting field [19], which is an overlap of physics, mathematics and computer science. It has achieved widespread interest in research community due to the remarkable characteristics of quantum physics like superposition phenomena and entanglement principle. It is considered that quantum computation will overcome the boundaries of classical computation due to the phenomenon of inherent quantum parallelism [5]. Starting with Richard Feynman [6], who first proposed the idea of quantum computer and attained considerable attention within the research community. Quantum computing has received much attention after Shor [23] proposal of integer numbers factorization in polynomial time and closely following that Grover [8] presented an algorithm for searching on quantum system, which exhibits quadratic swiftness when compared to its traditional counterparts used for the unsorted databases.

The astounding characteristics of quantum mechanics led to the emergence of many fields such as quantum based cryptography, quantum based steganography and quantum based image processing, to name a few. The classical image processing involves various complex algorithms used for the analysis and manipulation of digitized images and as the quantity and size of images is increasing rapidly due to the image sensing systems, it brings out the requirement of efficient and fast image-processing algorithms. Consequently, quantum image processing is developed to cope with the shortcomings in the area of classical image processing.

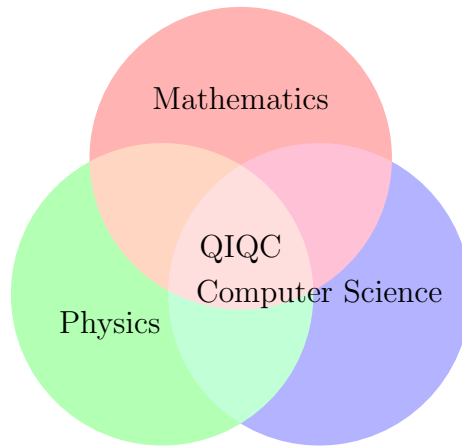


Figure 1.1: Quantum information and quantum computation

1.2 Brief overview of prior state of art

Recently, many quantum image representation (QIR) models for digital images are presented in the literature. Among these, the most well-known models are Qubit Lattice [28], Real Ket [14], Entangled Images [27], a flexible representation of quantum images (FRQI) [15], RGB MC representation for digital images (MCQI) [25], a novel enhanced quantum representation for digital images [33], and NQR of log-polar images [34]. In addition, various quantum digital image processing algorithms established on discrete cosine transforms, quantum wavelet transforms and geometric transforms are also presented in the literature which confirms the efficiency of these QIR models [3, 4, 7, 13].

1.3 Limitations of existing models

As compared to all existing QIR models, the FRQI and NEQR are seemed to be well-founded fundamental QIR models. In both models, a normalized quantum state represents the essential information about gray-scale and corresponding pixel's position of every pixel of digital image. An important aspect of these models is that unitary transforms can be applied at the same time on all pixels of the image by taking the advantage of superposition phenomenon of quantum mechanics. A limitation of the FRQI model is that it utilizes a single qubit for storing the gray-scale information of the image's pixels. As a result, the number of measurements required to accurately retrieve an image is very large. However, NEQR model addresses this problem of FRQI by storing the color information in a basis state of $2p$ -qubits in a

$2p$ -bit-deep image. This approach ensures the accurate retrieval of image information, but, it suffers from the space complexity as it does not utilize the superposition principle in color qubit sequence.

1.4 Problem statement and proposed solution

The problem statement is as follows: Even though FRQI and NEQR are well-known existing models used for storing and processing quantum images. But these models have some weaknesses especially they suffer from time and space complexity respectively. Therefore the need is to have some efficient model that have advantages of both existing models and improves the existing model FRQI.

This motivated to propose a QIR model that efficiently utilizes the superposition principle in the color qubit sequence and also ensures the accurate retrieval of image information in response to small number of measurements. The purpose of this work is twofold. Firstly, we establish that for an image of size $2^n \times 2^n$ with gray range 2^{2p} , the complexity of image preparation in FRQI model is $O(n2^{2n})$ which is linear. Secondly, we propose an improved flexible representation of quantum images (IFRQI) model that takes p qubits to captures gray-scale information of each pixel of a $2p$ -bit-deep image. The color information is encoded by employing rotation matrices corresponding to chosen values of angles which assist in accurate retrieval of original image information. The quantum image compression algorithm and basic image processing operations are discussed in detail in order to establish the effectiveness of IFRQI model. The performance analysis in respect of time and space complexity exhibits that the IFRQI model is comparable to FRQI and NEQR models.

1.5 Contributions

This research will primarily contribute to:

- Decrease the time complexity of famous FRQI model.
- Decrease the space complexity of NEQR model.
- Enhance the performance of existing models by presenting a new model IFRQI.

- Provides an efficient model for storing and retrieving digital images into quantum computer.
- Provides an efficient model for processing images into quantum computer.

Furthermore there are some secondary contributions as well, which are listed below.

- It can be used as a base framework for storing images in quantum image encryption strategies like [11, 16–18, 20, 26, 29, 30, 35–37].
- It can be used as a QIR model in quantum image steganography [9, 12].
- It can also be used in quantum image watermarking strategies like [22, 24, 32].
- It can be used in image scrambling [10, 38].

1.6 Organization of thesis

This thesis is divided into five chapters as described below. All the chapters provide the mandatory knowledge related to the proposed model and presents a complete aspect of the research.

Chapter 1. Introduction

This chapter provides the overview of background related to quantum information and quantum computation leading towards the quantum image processing. Following the background and motivation, the prior state of art is explained briefly along with the limitations of famous models NEQR and FRQI. From the limitation of existing famous models, we identified the problems and stated the problem statements accordingly. And then we have given the proposed solution in the same section of problem statements. The next section of this chapter gives the contributions of the proposed model. The contributions are classified into two types, primary contributions and secondary contributions and each one is elaborated briefly. And thesis organization is given at the end of this chapter.

Chapter 2. Background knowledge

This chapter presents the fundamental knowledge required for the understanding of proposed QIR model. Starting with basic concepts and definitions we cover almost all background knowledge related to quantum image representations in this chapter. Furthermore, some important mathematical knowledge required to understand the proposed research is also explained along with definitions and examples. The second half of chapter presents the strength or the power of quantum computer by stating the entanglement principle and four postulates of quantum mechanics.

Chapter 3. Literature review

This chapter gives a brief overview of the whole literature related to quantum image representation models. Moreover the famous QIR models (NEQR and FRQI) are explained in detail. The mathematical expression and an example image of these models are also discussed in this chapter.

Chapter 4. Methodology

This chapter has two main sections. The first section presents the analysis of FRQI and the second section describes the new model IFRQI in detail. Furthermore the basic image processing operations and quantum image compression are also given in the second section of this chapter.

Chapter 5. Conclusion

This chapter summarizes the main points of research that has been carried out in the thesis. And highlight the contributions of the proposed model in different fields of quantum image processing. The last section presents the potential future research work directions.

Chapter 2

Background knowledge

This chapter contains some basic notions and terminologies related to quantum computation and quantum information which are necessary for the understanding of this dissertation. The chapter consists of two sections: In first section, we discuss basic mathematical knowledge, while the entanglement principle and four postulates of quantum theory are discussed in the second section.

2.1 Basic mathematical knowledge

This section covers basic mathematical concepts such as complex field, vector space, inner product, Hilbert space, tensor product, qubit and Bra-Ket notation, and basic quantum operators. Also, the matrix representation of basic quantum operators and their circuit diagrams are discussed in this section.

Complex field

$z = a + ib$ defines the complex number, where a and b represents the real part and i represents the imaginary part, satisfying the condition $i^2 = -1$. \mathbb{C} denotes the set of all complex numbers and defined as $\mathbb{C} = a + ib$. If $n = a_0 + b_0i$, $m = a_1 + b_1i$ represents two complex numbers then these numbers can be added as, $n + m = (a_0 + a_1) + (b_0 + b_1)i$, and *multiplication* of $n = a_0 + b_0i$, $m = a_1 + b_1i$ is defined as $n \cdot m = (a_0a_1 - b_0b_1) + (a_0b_1 + a_1b_0)i$. The set of complex numbers \mathbb{C} has certain properties with respect to addition and multiplication, listed in Table 2.1, which make it a *field*. \bar{z} shows the *complex conjugate* of z , which is a complex number and it is of the form $z = a - bi$. While $|z|$ denotes its *magnitude* and is given by $\sqrt{a^2 + b^2}$.

Table 2.1: Properties of complex numbers

Property	Addition	Multiplication
Commutative	$n + m = m + n$	$n \cdot m = m \cdot n$
Associative	$(n + m) + p = n + (m + p)$	$(n \cdot m) \cdot p = n \cdot (m \cdot p)$
Identity element	$n + 0 = n$	$1 \cdot n = n = n \cdot 1$
Inverse element	$n + (-n) = 0 = (-n) + n$	$n \cdot n^{-1} = 1 = n^{-1} \cdot n$
Left distribution	$n \cdot (m + p) = n \cdot m + n \cdot p$	
Right distribution	$(n + m) \cdot p = n \cdot p + m \cdot p, \quad \forall n, m, p \in \mathbb{C}$	

Vector space (complex), its basis and dimension

Let V_c be a nonempty set with addition operation defined on it, and \mathbb{C} be the complex field. Then V_c is called a complex vector space if,

1. All elements of V_c satisfy commutative, associative, identity element and inverse element axioms w.r.t addition.
2. If there exists a mapping $\cdot : \mathbb{C} \times V_c \rightarrow C$, known as scalar multiplication, which satisfy
 - a) $1 \cdot v_0 = v_0$,
 - b) $c_0 \cdot (v_0 + v_1) = c_0 \cdot v_0 + c_0 \cdot v_1$ and,
 - c) $(c_0 + c_1)v_0 = c_0v_0 + c_1v_0$, for all $c_0, c_1 \in \mathbb{C}$ and $v_0, v_1 \in V_c$.

The elements of \mathbb{C} are known as *scalars* whereas the elements of V_c are known as *vectors*. $c_0v_0 + c_1v_1 + \dots + c_nv_n$ represents the linear combination of v_0, v_1, \dots, v_n , where v_0, v_1, \dots, v_n are known as vectors and c_0, c_1, \dots, c_n are called scalars. A subset $B = \{v_0, v_1, \dots, v_n\}$ of a vector's space V_c said to a *spanning (generating) set* of V_c if every vector of V_c can be presented as a sum of elements of B. If B is smallest (in respect of cardinality) spanning set of V_c , then it is called a *basis* of V_c and its cardinality (order) is called the *dimension* of V_c . In this dissertation, we shall deal only with finite d-dimensional complex vector spaces \mathbb{C}^d . The set $\{e_1 = (1, 0, \dots, 0), e_2 = (0, 1, \dots, 0), \dots, e_d = (0, 0, \dots, 1)\}$ forms a basis of \mathbb{C}^d , and known as standard basis of \mathbb{C}^d . Each vector v of \mathbb{C}^d has a representation as a d-tuple of the form $(\alpha_0, \alpha_1, \dots, \alpha_d)$, where each α_i is a complex number.

Inner product, orthonormal basis and hilbert space

If V_c represents complex vector space, then inner product is defined by the mapping $\langle \cdot | \cdot \rangle : V_c \times V_c \rightarrow \mathbb{C}$, a generalization of dot product of real vectors, if it obeys the following four axioms:

1. $\langle v_0 + v_1 | v_2 \rangle = \langle v_0 | v_2 \rangle + \langle v_1 | v_2 \rangle$
2. $\langle \alpha v_0 | v_1 \rangle = \alpha \langle v_0 | v_1 \rangle$
3. $\langle v_0 | v_1 \rangle = \overline{\langle v_1 | v_0 \rangle}$
4. $\langle v_0 | v_0 \rangle \geq 0$ and $\langle v_0 | v_0 \rangle = 0 \Leftrightarrow v_0 = 0$, for all $v_0, v_1, v_2 \in V_c$ and $\alpha \in \mathbb{C}$.

The existence of the inner product on V_c enables one to define *norm (length)* of each vector of V_c as follows:

$$\|v_c\| = \sqrt{\langle v_c | v_c \rangle}. \quad (2.1)$$

Note that $\|v_c\| \geq 0$ and $\|v_c\| = 0 \Leftrightarrow v_c = 0$. A vector v_c is called a *normalized* or *unit* vector if $\|v\| = 1$. Two vectors v_c and w_c are said to be *orthogonal* if $\langle v_c | w_c \rangle = 0$. B is an *orthonormal basis* of V_c , if vectors of B are orthogonal to each other and each element of B has norm 1. The standard basis of complex vector field \mathbb{C}^d defined previously is orthonormal basis. A finite dimensional space of vectors, if inner product defined on it, is known as a finite dimensional Hilbert space. However, infinite dimensional Hilbert spaces satisfy additional technical axiom which is not related to the work presented in this dissertation.

Qubit, bra-ket representation and tensor product spaces

Qubit stands for *quantum bit* and it is the fundamental unit of information about two-state (or two-level) physical systems of a single quantum particle. The spin of the electron and polarization of the photon are examples of two-state quantum physical systems. The spin up and spin down are taken as two states for the electron, while horizontal polarization and vertical polarization are taken as two-states for the photon. According to mathematical formulation, qubit can be represented as a vector in a two dimensional complex vector space \mathbb{C}^2 . In classical computers a bit can have only one state at a time either 0 or 1. Whereas, in quantum systems a qubit can have a coherent superposition (linear combination) of all possible states simultaneously, a property which is fundamental to quantum mechanics and quantum computing. We will use the term standard basis vectors interchangeably with computational basis states. A qubit state has the standard representation $|\psi\rangle$ used in the field of quantum mechanics, which is known as *ket*. The $|\cdot\rangle$ notation represents a vector and ψ is just a label. The computational basis states of \mathbb{C}^2 has ket representation as $|0\rangle = \begin{bmatrix} 1 \\ 0 \end{bmatrix}$ and $|1\rangle = \begin{bmatrix} 0 \\ 1 \end{bmatrix}$. A pure state of qubit is represented as $c_1|0\rangle + c_2|1\rangle$, where c_1 and c_2 are complex amplitudes

of basis states $|0\rangle$ and $|1\rangle$ resp., and satisfy the condition $|c_1|^2 + |c_2|^2 = 1$. The *dual vector* or *dual state* corresponding to state $|\psi\rangle$ is defined as the transpose of the complex conjugate of $|\psi\rangle$ and is denoted by $\langle\psi|$. Such that $\overline{|\psi\rangle}^t = \langle\psi| = |\psi\rangle^\dagger$. The row vector $\langle\psi|$ is known as *bra*. The mathematical structure used to study the quantum mechanics of multiparticle systems is known as *Tensor product Spaces*. Now we give the definition of a tensor product space. Assume that U_h and V_h are finite dimensional Hilbert spaces, with dimensions m and n respectively. Then $U_h \otimes V_h$ (read U_h tensor V_h) is an mn dimensional vector space defined as:

$$U_h \otimes V_h = \{\alpha_1 |u_1\rangle \otimes |v_1\rangle + \dots + \alpha_s |u_s\rangle \otimes |v_s\rangle : \alpha_t \in \mathbb{C}, |u_t\rangle \in U_h, |v_t\rangle \in V_h\} \quad (2.2)$$

An element $\alpha_1 |u_1\rangle \otimes |v_1\rangle + \dots + \alpha_s |u_s\rangle \otimes |v_s\rangle$ of $U_h \otimes V_h$ is actually a linear combination of ‘*tensor products*’ $|u_t\rangle \otimes |v_t\rangle$, where α_t s are scalars. In particular, if $B_U = \{|i\rangle : i = 0, 1, 2, \dots, m-1\}$ is the computational basis of U_h and $B_V = \{|j\rangle : j = 0, 1, 2, \dots, n-1\}$ is the computational basis of V , then $B_{U_h \otimes V_h} = \{|i\rangle \otimes |j\rangle\}$ is the computational basis of $U_h \otimes V_h$. We often use the abbreviated notations $|u\rangle |v\rangle$ or $|uv\rangle$ for the tensor product $|u\rangle \otimes |v\rangle$. For example, if $V = \mathbb{C}^2$ with basis vectors $|0\rangle$ and $|1\rangle$. Then the four vectors $|00\rangle, |01\rangle, |10\rangle, |11\rangle$ are the computational basis vectors of $V_h \otimes V_h = \mathbb{C}^2 \otimes \mathbb{C}^2$. And, $\mathbb{C}^2 \otimes \mathbb{C}^2 = \{c_{00} |00\rangle + c_{01} |01\rangle + c_{10} |10\rangle + c_{11} |11\rangle : c_{00}, c_{01}, c_{10}, c_{11} \in \mathbb{C}\}$. It is important to mention that the elements of $\mathbb{C}^2 \otimes \mathbb{C}^2$ represents the *joint states* of two qubits. The elements of tensor product space $U_h \otimes V_h$ satisfy the following axioms.

1. For scalar $c \in \mathbb{C}$ and vectors $u_0 \in U_h, v_0 \in V_h$,

$$c(|u_0\rangle \otimes |v_0\rangle) = (c|u_0\rangle) \otimes |v_0\rangle = |u_0\rangle \otimes (c|v_0\rangle). \quad (2.3)$$

2. For vectors $u_0, u_1 \in U_h$ and $v_0 \in V_h$,

$$(|u_0\rangle + |u_1\rangle) \otimes |v_0\rangle = |u_0\rangle \otimes |v_0\rangle + |u_1\rangle \otimes |v_0\rangle. \quad (2.4)$$

3. For vectors $u_0 \in U_h$ and $v_0, v_1 \in V_h$,

$$|u_0\rangle \otimes (|v_0\rangle + |v_1\rangle) = |u_0\rangle \otimes |v_0\rangle + |u_0\rangle \otimes |v_1\rangle \quad (2.5)$$

Linear operators, hermitian and unitary operators

Suppose U_h and V_h are two vector spaces. A function $F_l : U_h \rightarrow V_h$ is said to be a *linear operator* if it holds addition of vectors and multiplication of scalars, as given below.

1. For addition of vectors $|u_0\rangle, |u_1\rangle \in U_h$,

$$F_l |u_0 + u_1\rangle = F_l |u_0\rangle + L |u_1\rangle. \quad (2.6)$$

2. For scalar c , and vector $u_0 \in U_h$,

$$F_l |cu_0\rangle = cF_l |u_0\rangle. \quad (2.7)$$

We say F_l is a linear operator on V_h if $F_l : V_h \rightarrow V_h$. As an example, the *identity function* on V_h is a linear function denoted by I_V and defined as $I_V |v\rangle = |v\rangle, \forall |v\rangle \in V_h$. The *zero operator* on V_h denoted and defined as $\mathbf{0} |v_0\rangle = 0, \forall |v_0\rangle \in V_h$, is also a linear function. Linear operators between finite dimensional vector spaces has a simple and convenient *matrix representation*. If F_l is a linear function from m -dimension U_h (Hilbert space) to n -dimension V_h (Hilbert space), and $B_U = \{|i\rangle : i = 0, 1, 2, \dots, m-1\}$, $B_V = \{|j\rangle : j = 0, 1, 2, \dots, n-1\}$ are computational basis of U_h and V_h respectively. Then, the matrix representation of F_l is $[F_{ji}]_{n \times m}$, where $F_{ji} = \langle j|F|i\rangle$ (inner product between $|j\rangle$ and $L|i\rangle$) is the entry at j th row and i th column of matrix $[F_{ji}]_{n \times m}$. Moreover, each matrix is a linear operator. And the identity matrix represents the associated identity operator on vector space V_h . A matrix U_h is known as *Hermitian matrix* if $\overline{U_h}^t = U_h = U_h^\dagger$, that is, the transpose of complex conjugate of U_h is equal to U_h . And, a matrix U_h is called *unitary* if $U_h U_h^\dagger = U_h^\dagger U_h = I$, that is, the inverse of U_h is U_h^\dagger . Similarly, a linear operator is called Hermitian (unitary) operator between Hilbert spaces U_h and V_h if the associated matrix is a Hermitian (unitary) matrix. If Q and R are linear operators on U_h and V_h resp., then $Q \otimes R$, defined as in Eq. (.), is a linear operator on $U_h \otimes V_h$. And, if Q, R are Hermitian (unitary) operators then so is $Q \otimes R$.

$$Q = \begin{bmatrix} q_{11} & q_{12} & \cdots & q_{1m} \\ q_{21} & q_{22} & \cdots & q_{2m} \\ \vdots & \vdots & \ddots & \vdots \\ q_{m1} & q_{m2} & \cdots & q_{mm} \end{bmatrix}, R = \begin{bmatrix} r_{11} & r_{12} & \cdots & r_{1n} \\ r_{21} & r_{22} & \cdots & r_{2n} \\ \vdots & \vdots & \ddots & \vdots \\ r_{n1} & r_{n2} & \cdots & r_{nn} \end{bmatrix} \quad (2.8)$$

$$Q \otimes R = \begin{bmatrix} q_{11}R & q_{12}R & \cdots & q_{1m}R \\ q_{21}R & q_{22}R & \cdots & q_{2m}R \\ \vdots & \vdots & \ddots & \vdots \\ q_{m1}R & q_{m2}R & \cdots & q_{mm}R \end{bmatrix} \text{ where } q_{ij}R \text{ are submatrices.} \quad (2.9)$$

Outer product operator, completeness relation, projection operator

Suppose V_h is an n -dimension Hilbert space and $|\psi\rangle = [\alpha_1 \ \alpha_2 \ \dots \ \alpha_n]^t$ is a vector of V . The *outer product* operator $|\psi\rangle\langle\psi| : V \rightarrow V$ is a linear operator defined as,

$$(|\psi\rangle\langle\psi|)(|v\rangle) \equiv |\psi\rangle\langle\psi|v\rangle = \langle\psi|v\rangle|\psi\rangle, \forall |v\rangle \in V. \quad (2.10)$$

The matrix representation of outer product operator $|\psi\rangle\langle\psi|$ is given as in Eq. (2.11).

$$|\psi\rangle\langle\psi| = \begin{bmatrix} \alpha_1 \\ \alpha_2 \\ \vdots \\ \alpha_n \end{bmatrix} \begin{bmatrix} \bar{\alpha}_1 & \bar{\alpha}_2 & \dots & \bar{\alpha}_n \end{bmatrix} = \begin{bmatrix} \alpha_1\bar{\alpha}_1 & \alpha_1\bar{\alpha}_2 & \dots & \alpha_1\bar{\alpha}_n \\ \alpha_2\bar{\alpha}_1 & \alpha_2\bar{\alpha}_2 & \dots & \alpha_2\bar{\alpha}_n \\ \vdots & \vdots & \ddots & \vdots \\ \alpha_n\bar{\alpha}_1 & \alpha_n\bar{\alpha}_2 & \dots & \alpha_n\bar{\alpha}_n \end{bmatrix} \quad (2.11)$$

Suppose $B = \{|v_1\rangle, |v_2\rangle, \dots, |v_n\rangle\}$ is an orthonormal basis of V_h . Then, every arbitrary vector v in V_h can be expressed as, $v = c_0v_0 + c_1v_1 + \dots + c_{n-1}v_{n-1}$, for some scalars c_0, c_1, \dots, c_{n-1} . Using the fact that $\langle v_0|v\rangle = c_0, \dots, \langle v_{n-1}|v\rangle = c_{n-1}$, we have,

$$\left(\sum_{i=0}^{n-1} |v_i\rangle\langle v_i| \right) |v\rangle = \sum_{i=0}^{n-1} \langle v_i|v\rangle |v_i\rangle = \sum_{i=0}^{n-1} c_i |v_i\rangle = |v\rangle, \forall v \in V_h. \quad (2.12)$$

Consequently we have the *completeness relation* given as in Eq. (2.13).

$$\sum_{i=0}^{n-1} |v_i\rangle\langle v_i| = I_V. \quad (2.13)$$

For each $i = 0, 2, \dots, n-1$, the linear operator $|v_i\rangle\langle v_i|$ is known as *projection operator*. The process of applying a projection operator on a quantum state is known as *projective measurement*. Note that for the computational basis $\{|i\rangle\}$ of V_h , $|i\rangle\langle i|$ denotes the projection operators, and completeness relation takes the form as $\sum_{i=0}^{n-1} |i\rangle\langle i| = I$.

Basic quantum gates, their matrix representation and circuit diagrams

We conclude this section with listing some basic quantum gates, their circuit diagrams and matrix representations as in Fig. 2.1.

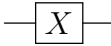
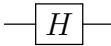
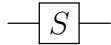
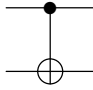
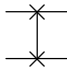
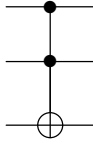
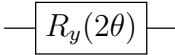
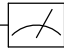

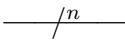
Gate	Circuit diagram	Matrix representation
<i>NOT</i>		$\begin{bmatrix} 0 & 1 \\ 1 & 0 \end{bmatrix}$
<i>Hadamard</i>		$\frac{1}{\sqrt{2}} \begin{bmatrix} 1 & 1 \\ 1 & -1 \end{bmatrix}$
<i>Phase</i>		$\begin{bmatrix} 1 & 0 \\ 0 & i \end{bmatrix}$
<i>Controlloed-NOT</i>		$\begin{bmatrix} 1 & 0 & 0 & 0 \\ 0 & 1 & 0 & 0 \\ 0 & 0 & 0 & 1 \\ 0 & 0 & 1 & 0 \end{bmatrix}$
<i>Swap</i>		$\begin{bmatrix} 1 & 0 & 0 & 0 \\ 0 & 0 & 1 & 0 \\ 0 & 1 & 0 & 0 \\ 0 & 0 & 1 & 1 \end{bmatrix}$
<i>Toffoli</i>		$\begin{bmatrix} 1 & 0 & 0 & 0 & 0 & 0 & 0 & 0 \\ 0 & 1 & 0 & 0 & 0 & 0 & 0 & 0 \\ 0 & 0 & 1 & 0 & 0 & 0 & 0 & 0 \\ 0 & 0 & 0 & 1 & 0 & 0 & 0 & 0 \\ 0 & 0 & 0 & 0 & 1 & 0 & 0 & 0 \\ 0 & 0 & 0 & 0 & 0 & 1 & 0 & 0 \\ 0 & 0 & 0 & 0 & 0 & 0 & 0 & 1 \\ 0 & 0 & 0 & 0 & 0 & 0 & 0 & 1 \end{bmatrix}$
<i>Rotation</i>		$\begin{bmatrix} \cos \theta & -\sin \theta \\ \sin \theta & \cos \theta \end{bmatrix}$
<i>meter</i>		Projection onto $ 0\rangle$ and $ 1\rangle$
<i>qubit</i>		wire carrying a single qubit
<i>n qubits</i>		wire carrying n qubits

Figure 2.1: Basis quantum gate, their circuit diagrams and matrix representations

2.2 Strength of quantum computer

The strength of quantum computation is the superposition principal. Superposition principal states a qubit can exist in all possible states following the normalization constraint. Like a qubit can have a state 0 or 1 and both 0 and 1 at the same time. A classical bit can store only single piece of information whereas a quantum bit can store unlimited information.

Classical computations are irreversible while quantum computations are reversible. It means in classical computations looking to output we cannot predict what inputs were whereas in quantum looking to the output we can predict what the inputs were. Because quantum computations are based on quantum gates and quantum gates are unitary in nature. This makes the quantum computers more powerful.

2.2.1 Entanglement

Entanglement is the property that is defined by an entangled state. If a composite quantum system is in such a state that it cannot be split into the tensor product of component systems then it is called an entangled state.

2.2.2 Quantum mechanics's postulates

Four quantum mechanics's postulates are as follows:

1. Any physical quantum system lies in a complex space of vectors with inner product is called the state space of that quantum system. A physical system can be presented in the form of its state vector of state space.
2. The development of a quantum system which is closed is delineated by the unitary transforms.
3. The probability of measurement of a quantum system having a sure result is ascertained by the complex amplitude of its basis vectors. Once the measurement is done, superposition collapses and system remains in the measured state.
4. The vector space of a composite system of quantum can be shown by the tensor product of its component systems' vector spaces.

Chapter 3

Literature Review

In recent years, quantum image processing has gained widespread interest in research community due to the remarkable characteristics such as entanglement and superposition of quantum mechanics. The quantum image processing is a technique, which utilizes methods based on quantum mechanics to improve the classical image processing.

Quantum image representations are the models that are used to store digital images on to the quantum systems. The QIR models are broadly classified in two types as listed below.

1. QIR for grey-scale images
2. QIR models for color images

We primarily deal with grey-scale images that's why we will see it in depth but before that a brief overview of color images is also presented.

3.1 QIR models for color images

In this section we briefly review some famous quantum image representation (QIR) models for color images, their features and mathematical expressions. Some famous QIR models for color images are

MCQI RGB multi-channel representation for images [25]

QMCR Red green blue multi-channel quantum representations of digital images [1]

NCQI A novel quantum representation of color digital images [21]

QRCI A new quantum representation model of color images [31]

3.1.1 The MCQI Representation

The MCQI model [25] encodes the color and their pixels's positions of an image in $2n + 3$ normalized qubits. The Mathematical expression of the model is shown in

$$|I_m cqi\rangle = \frac{1}{2^m + 1} \sum_{i=0}^{2^{2m}-1} |C_{RGBi}\rangle |i\rangle. \quad (3.1)$$

The above expression has two parts. The first part is used to encode color information of three angels $\theta_{Ri}\theta_{Gi}\theta_{Bi}$ where the second part captures the corresponding position values of pixels.

3.1.2 The QMCR model

In this model the digital color images are stored in a two entangled sequences of qubits. The first qubit sequence stores the Red-Green-Blue color information of pixels while the second sequence is used to store position information. The mathematical representation of image is given below.

$$|I\rangle = \frac{1}{2^n} \sum_{i=0}^{2^{2n}-1} |C_{RGBi}\rangle |i\rangle. \quad (3.2)$$

where $|C_{RGBi}\rangle$ is used to store RGB color information and $|C_{RGBi}\rangle = |C_{Ri}\rangle |C_{Gi}\rangle |C_{Bi}\rangle$. And i stores the position information of pixels of image.

3.1.3 The NCQI representation

A novel quantum representation of color digital images [21] is presented in 2016. This model captures the RGB color values into the basis state of color qubits. The formula of NCQI is presented in

$$|I_n cqi\rangle = \frac{1}{2^n} \sum_{j=0}^{2^{2n}-1} |C(j)\rangle |j\rangle. \quad (3.3)$$

where $C(j)$ stores the color information of pixels at position i .

3.1.4 The QRCI representation

Following the NCQI, a new quantum representation model of color digital images captures the essential information of colors into the basis states of

$2n + 6$ qubits for an image of size $2^n \times 2^n$. The QRCI image is represented as

$$|I\rangle = \frac{1}{\sqrt{2^{2n} + 3}} \sum_{L=0}^{2^3-1} \sum_{i=0}^{2^{2n}-1} |C_L(i)\rangle |Li\rangle. \quad (3.4)$$

where $|C_L(i)\rangle = |R_{Li}G_{Li}B_{Li}\rangle$.

3.2 QIR models for grey-scale images

Some famous quantum image representation (QIR) models their features and mathematical expressions are presented in this section. For the gray-scale images the famous QIR models are

- Qubit lattice
- Entangled image
- Real ket
- FRQI
- NEQR

3.2.1 Qubit lattice

Venegas Andraca and Bose [28] presented qubit lattice a quantum image model for the first time. They [28] defined a machine that detects and records electromagnetic waves of different frequencies, and produces initialized qubits. In this way, color is stored in a qubit by detecting different frequencies, and translating them to different quantum states. Every pixel of image takes single qubit for storage and the entire image is encoded in the form of a qubit matrix.

3.2.2 Real ket

After the two years of Qubit Lattice, Latorre [14] proposed a new quantum representation model for quantum images named as Real Ket. In Real Ket, color value of every pixel is represented in coefficients of basis state, which are qubit sequences of four-dimensions.

θ_0 00	θ_1 01
θ_2 10	θ_3 11

$$\begin{aligned}
|i\rangle &= \frac{1}{2}[(\cos \theta_0 |0\rangle + \sin \theta_0 |1\rangle) \otimes |00\rangle + (\cos \theta_1 |0\rangle + \sin \theta_1 |1\rangle) \otimes |01\rangle \\
&\quad + (\cos \theta_2 |0\rangle + \sin \theta_2 |1\rangle) \otimes |10\rangle + (\cos \theta_3 |0\rangle + \sin \theta_3 |1\rangle) \otimes |11\rangle] \\
&= \frac{1}{2}[(\cos \theta_0 |0\rangle + \sin \theta_0 |1\rangle) \otimes |0\rangle + (\cos \theta_1 |0\rangle + \sin \theta_1 |1\rangle) \otimes |1\rangle \\
&\quad + (\cos \theta_2 |0\rangle + \sin \theta_2 |1\rangle) \otimes |2\rangle + (\cos \theta_3 |0\rangle + \sin \theta_3 |1\rangle) \otimes |3\rangle]
\end{aligned}$$

Figure 3.1: An example image with its FRQI state

3.2.3 Entangled image

In 2009, Venegas-Andraca [27] proposed Entangled Image model for processing images in a quantum system using the peculiar property (i.e., entanglement) of quantum mechanics. This model is similar to previous QIR model (Qubit lattice) of Venegas-Andraca in addition, it takes advantage of entanglement property of quantum mechanics for representing relationship between pixels so that the image retrieval is possible without any use of additional information.

3.2.4 FRQI

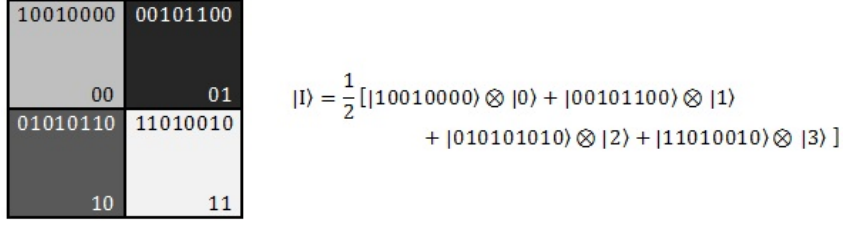
Le et al. [15] took a new look at quantum image processing and proposed a flexible representation of quantum images (FRQI). The mathematical state of FRQI for a $2^n \times 2^n$ image is presented as:

$$|I_{frqi}\rangle = \frac{1}{2^m} \sum_{j=0}^{2^{2m}-1} (\cos \theta_j |0\rangle + \sin \theta_j |1\rangle) \otimes |j\rangle. \quad (3.5)$$

FRQI captures gray-scale color values and their corresponding positions of pixels, and store them in a normalized state. For each pixel, FRQI model stores its gray-scale information into a single qubit by using an angle θ and its position information into a $2n$ -dimensional qubit sequence. Color qubit of FRQI is entangled with $2n$ -dimensional qubit sequence which stores positional information. The example of FRQI image is shown in Fig. 3.1. The FRQI representation can also be expressed as in (3.6):

$$|I\rangle = \frac{1}{2^m} \sum_{j=0}^{2^{2m}-1} (\alpha_j |0\rangle + \beta_j |1\rangle) \otimes |j\rangle. \quad (3.6)$$

where $\alpha_j = \cos \theta_j$ and $\beta_j = \sin \theta_j$, for all $0 \leq j \leq 2^{2m} - 1$.

Figure 3.2: A 2×2 image and its NEQR state

3.2.5 NEQR

More recently, Z, Yi and Lu. [33] proposed a novel enhanced quantum representation of digital images. It takes $q + 2n$ qubits to store $2^m \times 2^m$ quantum image for gray intensities 2^q , and represented as:

$$|I\rangle = \frac{1}{2^m} \sum_{j=0}^{2^{2m}-1} |(f(j))|j\rangle. \quad (3.7)$$

The NEQR takes two sequences of entangled qubits, for storing gray-scale information and pixel's position of the image, and it stores positions as well as colors of all pixels of an image into the basis states. The example NEQR image is shown in Figure 3.2.

As mentioned by Zhang, Yi and Lu [33], Entangled Image and Qubit lattice is quantum counterpart of classical image representation models, without any significant performance improvement than all other image representation models. Whereas the Real Ket, FRQI, and NEQR are based on the phenomenon of superposition thus they can process quantum operations for full image simultaneously. So far, compared to all existing models FRQI and NEQR exhibit more performance improvement, and considered to be useful quantum image representation models. But these approaches also have some limitations. A drawback of FRQI is that it uses only one qubit for storing the color information of each pixel. As a result, the number of measurements required to accurately retrieve an image are very large. However, NEQR model addresses this problem of FRQI by storing the color information in a basis state of $2p$ -qubits in a $2p$ -bit-deep image. This approach ensures the accurate retrieval of image information, but, it suffers from the space complexity as it does not utilize the superposition principle in color qubit sequence. This motivated us to propose a QIR model that efficiently utilizes the superposition principle in the color qubit sequence and also ensures the accurate retrieval of image information in response to small number of measurements.

Chapter 4

Methodology

In this chapter, first of all we present analysis of FRQI model and after that we discuss the proposed QIR model improved flexible representation of quantum images (IFRQI) in detail. In Analysis of FRQI, we discuss the time complexity of famous QIR model FRQI and how to reduce it with the help of ancillary qubits. In the next main section the IFRQI, image processing operators and quantum image compression algorithm is presented.

4.1 Analysis of FRQI

In [15], Le et al. established that the time complexity - the number of basic operations required to turn the initialized state to FRQI state - for the FRQI model is $O(2^{4n})$ for an image of size $2^n \times 2^n$. This is quadratic in the size of image. However, in this section we prove that the complexity of FRQI model can be significantly reduced to be linear in the size of an image.

To begin with introducing some basic notations and concepts. A matrix whose inverse is same as its Hermitian conjugate or its adjoint is called a unitary matrix. Each quantum transformation has representation as unitary matrix. For this reason, quantum transformations are often called unitary transformations. For a unitary matrix

$$U = \begin{bmatrix} u_{00} & u_{01} \\ u_{10} & u_{11} \end{bmatrix}$$

where $m \in \{0, 1, 2, \dots\}$ and set the $(m + 1)$ bit transformation $C^m(U)$ as,

$$C^m(U)(|c_1, \dots, c_m, d\rangle) = \begin{cases} u_{0d} |c_1, \dots, c_m, 0\rangle + u_{1d} |c_1, \dots, c_m, 1\rangle & \text{if } \bigwedge_{k=1}^m c_k = 1 \\ |c_1, \dots, c_m, d\rangle & \text{if } \bigwedge_{k=1}^m c_k = 0 \end{cases}$$

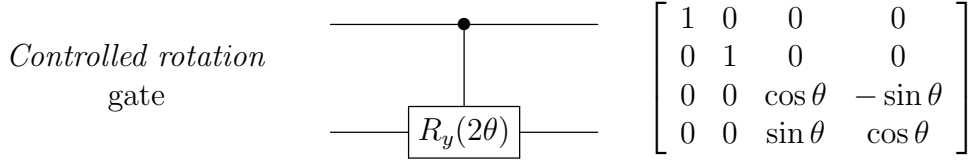
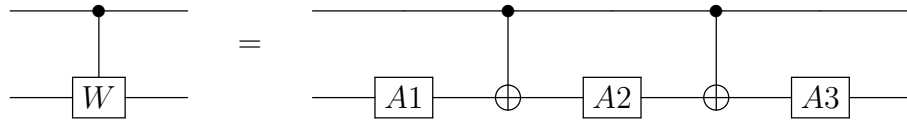


Figure 4.1: Controlled rotation gate $C^1(R_y(2\theta))$.

for all $c_1, c_2, \dots, c_m, d \in \{0, 1\}$ and $\bigwedge_{k=1}^m c_k = 1$ denotes the AND of the Boolean variables $\{c_k\}$. The transformation $C^m(U)$ is called a generalized-Toffoli gate and family of all $C^0(U)$ together with $C^1(X)$, where $X = \begin{bmatrix} 0 & 1 \\ 1 & 0 \end{bmatrix}$, is called family of basic operations or basic gates [2]. The Hadamard gate is as $H = \frac{1}{\sqrt{2}} \begin{bmatrix} 1 & 1 \\ 1 & -1 \end{bmatrix}$. The gate notation and matrix representation of controlled rotation gate $C^1(R_y(2\theta))$, is shown in Fig. 4.1. A 2×2 matrix U is called special unitary if its determinant is 1. The $SU(2)$ represents the special unitary matrices's set of the size 2×2 . The following Lemma determines the complexity of $C^1(W)$, where $W \in SU(2)$.

Lemma 1 ([2], Lemma 5.1) *For a special unitary 2×2 matrix W , a quantum operation $C^1(W)$, can be applied by a circuit of the type*



where $A1, A2, \text{ and } A3 \in SU(2), \Leftrightarrow W \in SU(2)$.

Remark 1 *The time complexity of quantum operation $C^1(R_y(2\theta))$ is at most 5.*

The following result gives the complexity of $C^2(U)$, which is a unitary matrix.

Lemma 2 ([2]) *For a unitary 2×2 matrix U , a quantum operation $C^2(U)$ can be decomposed into at most sixteen basic operations: eight 1-bit operations (C^0) and eight CNOT operations ($C^1(X)$).*

The following result gives the complexity of $C^m(U)$, where U represents a unitary matrix of size 2×2 and $m \geq 3$.

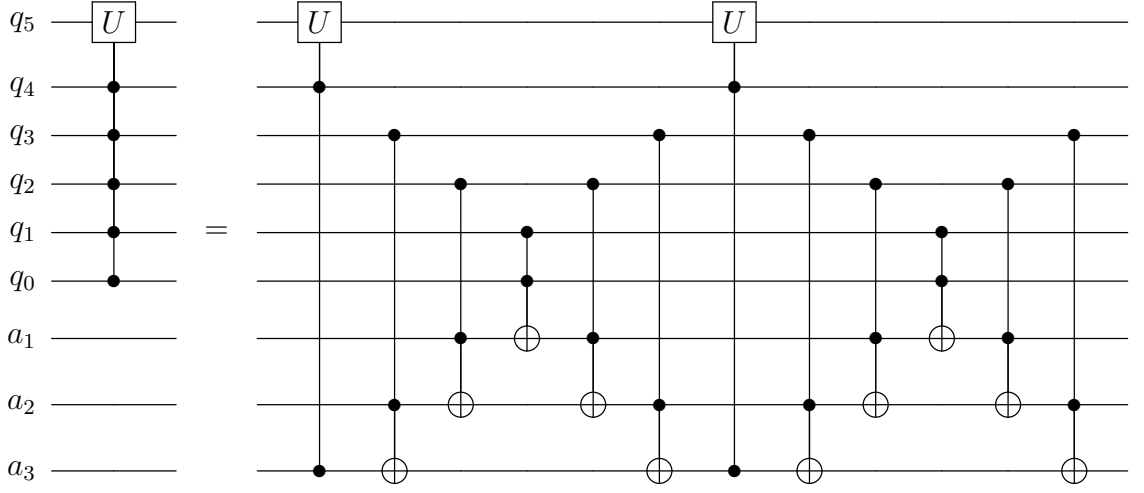


Figure 4.2: The decomposed quantum circuit for $C^5(U)$; q_0 to q_5 are operating qubits, while a_1 to a_3 are supporting qubits

Lemma 3 *Given $m \in \{3, 4, \dots\}$. The quantum operation $C^m(U)$ can be decomposed, into $4m - 10$ quantum operations $C^2(X)$ and 2 quantum operations $C^2(U)$, provided that $m - 2$ ancillary qubits are present.*

The above Lemma is a generalization of Lemma 7.2 in [2]. Figure 4.2 shows an example of decomposition of quantum operation $C^5(U)$ with the help of three supporting qubits.

Corollary 1 *The time complexity of $C^m(R_y(2\theta))$ is $O(m)$, provided that enough ancillary qubits are present.*

Proof 1 *From the Lemma 2 and Lemma 3, the result follows.*

The Lemma 1 in [15] provides the existence of a unitary transformation $\mathcal{P} = \mathcal{R} \circ \mathcal{H}$, that changes the initialized state to final state of FRQI. The components \mathcal{H} and \mathcal{R} , of \mathcal{P} are given in Eq. (4.1).

$$\mathcal{H} = I \otimes H^{\otimes 2n}, \quad \mathcal{R} = \prod_{i=0}^{2^{2n}-1} R_i \quad (4.1)$$

In Eq. (4.1), I is identity matrix, H is the Hadamard matrix and R_i is the controlled rotation matrix defined as in Eq. (4.2), for each i in $\{0, 1, \dots, 2^{2n} - 1\}$.

$$R_i = \left(I \otimes \sum_{j=0, j \neq i}^{2^{2n}-1} |j\rangle \langle j| \right) + R_y(2\theta_i) \otimes |i\rangle \langle i| \quad (4.2)$$

We conclude the analysis with the following theorem on the complexity of image preparation phase of FRQI, subject to the assumption that there are sufficient supporting qubits available.

Theorem 1 *The complexity of preparing FRQI state of a $2^n \times 2^n$ gray-scale image, is $O(n2^{2n})$.*

Proof 2 *As the unitary transform $\mathcal{P} = \mathcal{H} \circ \mathcal{R}$ decomposes into \mathcal{H} and \mathcal{R} given in (4.1), the time complexity of \mathcal{H} is $2n$. By using Lemma 2 and Lemma 3, and the fact that the quantum transform \mathcal{R} is a product of 2^{2n} controlled rotations R_i (i.e., $C^{2n}(R_y(2\theta_i))$), it follows that the time complexity of \mathcal{R} is at most $2^{2n}(128n - 128)$. Thus, the time complexity of \mathcal{P} is at most $2^{2n}(128n - 128) + 2n$, or equivalently $O(n2^{2n})$. This concludes the proof of the theorem.*

4.2 An improved flexible representation of quantum images

Through the analysis of FRQI and NEQR image models, it is evident that the main advantage of these models results from utilization of superposition principal in qubits that represents position information of whole image's pixels, due to which all pixels can be operated at the same time. On the other hand, the major limitation of FRQI is the use of just one qubit to represent the color values of all pixels. While the NEQR takes $2p$ qubits to encode the color values of a pixel with $2p$ -bit depth and hence do not incorporate the advantage of superposition principal in this part. To completely incorporate the benefit of superposition principal, proposed IFRQI model takes two qubit sequences which are entangled, to store the entire image in the superposition. In IFRQI model, the first sequence comprising of p qubits are employed to capture the color (gray-scale) values of each pixel of $2p$ -bit depth, while the second sequence of qubits is used to store position information of each pixel.

If the intensity of image is 2^{2p} , and $f(i) = P_i^{2^{2p-1}} P_i^{2^{2p-2}} \dots P_i^1 P_i^0$ is the color information of the corresponding pixel at the i th position where $P_i^j \in \{0, 1\}$ for all $j \in \{0, 1, \dots, 2p-1\}$. The ordering of pixels positions of a 4×4 image is given in Fig. 4.3. By encoding the 2 -bit information $P_i^{2^{k+1}} P_i^{2^k}$ via the angle θ_k , chosen by the rule given in Table 4.1, we obtain the qubit $\alpha_{i,k} |0\rangle + \beta_{i,k} |1\rangle$, where $\alpha_{i,k} = \cos \theta_k$ and $\beta_{i,k} = \sin \theta_k$ for all $0 \leq k \leq p-1$. Therefore, the joint state of p qubits, $\bigotimes_{k=0}^{p-1} (\alpha_{i,k} |0\rangle + \beta_{i,k} |1\rangle)$, represents the gray-scale information $f(i)$, in IFRQI state, of the its pixel at i th position. The IFRQI

0	1	2	3
4	5	6	7
8	9	10	11
12	13	14	15

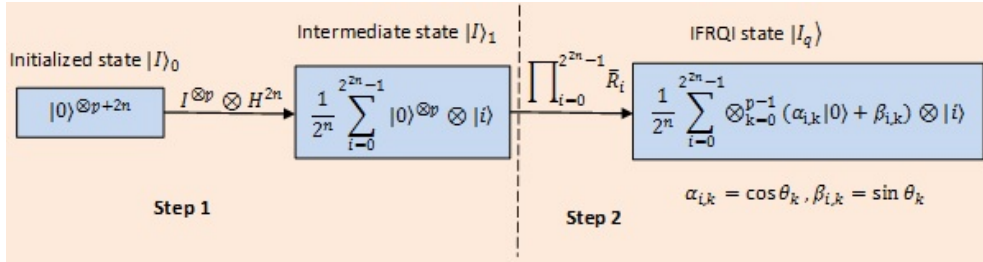
Figure 4.3: The ordering of pixels positions of a 4×4 image

Figure 4.4: Quantum image preparation process of IFRQI model

state of digital image I_c is

$$|I_q\rangle = \frac{1}{2^n} \sum_{i=0}^{2^{2n}-1} \otimes_{k=0}^{p-1} (\alpha_{i,k} |0\rangle + \beta_{i,k} |1\rangle) \otimes |i\rangle. \quad (4.3)$$

Where $\alpha_{i,k} = \cos \theta_k$, $\beta_{i,k} = \sin \theta_k$ for all $0 \leq k \leq p-1$.

Table 4.1: Proposed method for encoding 2-bit information

$P_i^{2k+1} P_i^{2k}$	00	01	10	11
θ_k	0	$\frac{\pi}{5}$	$\frac{\pi}{2} - \frac{\pi}{5}$	$\frac{\pi}{2}$

4.2.1 Quantum image preparation

The process of image preparation of proposed scheme is given in Fig. 4.4. The process starts with preparing initialized quantum states. Then, these states are transformed to desired quantum states using unitary transformations. For this purpose, we consider a classical image I_c of size $2^n \times 2^n$ with gray range 2^{2p} , which has its IFRQI state I_q of $p+2n$ qubits.

We start with preparing and initializing $p+2n$ qubits. The preliminary state is shown as in (4.4):

$$|I\rangle_0 = |0\rangle^{\otimes(p+2n)}. \quad (4.4)$$

From state $|I\rangle_0$, the IFRQI state I_q can be obtained by dividing the quantum image preparation phase mainly into two steps.

Step 1:

In this step, we apply the quantum operation U_1 , given in (4.5), on preliminary state $|I\rangle_0$ and obtain the state $|I\rangle_1$, given in (4.6).

$$U_1 = I^{\otimes p} \otimes H^{\otimes 2n} \quad (4.5)$$

$$\begin{aligned} U_1(|I\rangle_0) &= (I^{\otimes p} \otimes H^{\otimes 2n})(|0\rangle^{\otimes(p+2n)}) \\ &= \frac{1}{2^n} (I|0\rangle)^{\otimes p} \otimes (H|0\rangle)^{\otimes 2n} \\ |I\rangle_1 &= \frac{1}{2^n} |0\rangle^{\otimes p} \otimes \sum_{i=0}^{2^{2n}-1} |i\rangle \end{aligned} \quad (4.6)$$

Step 2:

In this step, we apply 2^{2n} quantum sub-operations to encode pixel's color information. Particularly, the quantum sub-operation \bar{R}_i , given in (4.7), is used to set the color value for the pixel at i th position.

$$\bar{R}_i = \left(I^{\otimes p} \otimes \sum_{j=0, j \neq i}^{2^{2n}-1} |j\rangle \langle j| \right) + L_i \otimes |i\rangle \langle i| \quad (4.7)$$

where L_i is a quantum operation as given in (4.8):

$$L_i = \otimes_{k=0}^{p-1} L_i^k \quad (4.8)$$

Since p qubits represent the color information in IFRQI, therefore, L_i is decomposed into p number of operations presented in (4.9):

$$L_i^k = R_y(2\theta_k) \quad (4.9)$$

where $R_y(2\theta_k)$ is the unitary matrix representing the rotation about \hat{y} axis by the angle θ_k .

From (4.9), if $\theta_k \neq 0$, then L_i^k is a generalized-controlled rotation $C^{2n}(R_y(2\theta_k))$, as a component in (4.7). Otherwise, it is identity matrix whose application has no effect on the quantum state. Accordingly, the operation L_i stores

color information for the pixel at i th position. Application of \overline{R}_i on the intermediate state $|I\rangle_1$ yields (4.10):

$$\begin{aligned}
\overline{R}_i |I\rangle_1 &= \overline{R}_i \left(\frac{1}{2^n} \sum_{j=0}^{2^{2n}-1} |0\rangle^{\otimes p} |j\rangle \right) \\
&= \left(I^{\otimes p} \otimes \sum_{j=0, j \neq i}^{2^{2n}-1} |j\rangle \langle j| + L_i \otimes |i\rangle \langle i| \right) \left(\frac{1}{2^n} \sum_{j=0}^{2^{2n}-1} |0\rangle^{\otimes p} |j\rangle \right) \\
&= \frac{1}{2^n} \left[\left(I^{\otimes p} \otimes \sum_{j=0, j \neq i}^{2^{2n}-1} |j\rangle \langle j| \right) \left(\sum_{j=0}^{2^{2n}-1} |0\rangle^{\otimes p} |j\rangle \right) \right. \\
&\quad \left. + \left(L_i \otimes |i\rangle \langle i| \right) \left(\sum_{j=0}^{2^{2n}-1} |0\rangle^{\otimes p} |j\rangle \right) \right] \\
&= \frac{1}{2^n} \left[\sum_{j=0, j \neq i}^{2^{2n}-1} |0\rangle^{\otimes p} |j\rangle + L_i |0\rangle^{\otimes p} \otimes |i\rangle \right] \\
&= \frac{1}{2^n} \left[\sum_{j=0, j \neq i}^{2^{2n}-1} |0\rangle^{\otimes p} |j\rangle + \left(\otimes_{k=0}^{k=p-1} L_i^k \right) (|0\rangle^{\otimes p}) \otimes |i\rangle \right] \\
&= \frac{1}{2^n} \left[\sum_{j=0, j \neq i}^{2^{2n}-1} |0\rangle^{\otimes p} |j\rangle + \left(\otimes_{k=0}^{k=p-1} (\alpha_{i,k} |0\rangle + \beta_{i,k} |1\rangle) \right) \otimes |i\rangle \right] \tag{4.10}
\end{aligned}$$

Since i ranges from 0 to $2^{2n} - 1$, therefore, the application of composite transform $U_2 = \prod_{i=0}^{2^{2n}-1} \overline{R}_i$ on $|I\rangle_1$ produces the IFRQI state, given in Eq. (4.11).

$$|I_q\rangle = \frac{1}{2^n} \sum_{i=0}^{2^{2n}-1} \left(\bigotimes_{k=0}^{p-1} (\alpha_{i,k} |0\rangle + \beta_{i,k} |1\rangle) \right) \otimes |i\rangle \tag{4.11}$$

Now, we discuss the time complexity of the image preparation phase. As described above, the image preparation phase consists of two steps. From (4.5), it is clear that the complexity of the first step is $O(p + 2n)$. And, the second step in image preparation phase is the composition of 2^{2n} operations \overline{R}_i , where $i = 0, 1, \dots, 2^{2n} - 1$. In order to determine the complexity of second step, the complexity of the operation \overline{R}_i is first discussed. The following Lemma summarises the complexity of R_i .

Lemma 4 *The time complexity of the transformation \overline{R}_i , given in (4.7), is $O(pn)$ provided that enough supporting qubits are present.*

Proof 3 The transformation \overline{R}_i sets the gray-scale information of the pixel at i th position in the first sequence of p qubits of quantum state $|I\rangle_1$. And, color information setting constituent L_i in \overline{R}_i performs p sub-operations L_i^k for each $k \in \{0, 1, 2, \dots, p-1\}$, where each L_i^k is a rotation $R_y(2\theta_k)$ about \hat{y} axis by the angle θ_k . Thus, the transformation \overline{R}_i can be represented as in (4.12)

$$\overline{R}_i = \prod_{k=0}^{p-1} C^{2n}(R_y(2\theta_k)) \quad (4.12)$$

If $P_i^{2k+1}P_i^{2k} = 00$ for $k \in \{0, 1, 2, \dots, p-1\}$, then $\theta_k = 0$. Thus, $L_i^k = R_y(2\theta_k) = R_y(0) = I$ is the identity operation, and the corresponding constituent $C^{2n}(R_y(2\theta_k))$ in (4.12) is also the identity operation. On the other hand, if, $P_i^{2k+1}P_i^{2k} \neq 00$ for $k \in \{0, 1, 2, \dots, p-1\}$, then $\theta_k \neq 0$ and its value is chosen from Table 1. Thus, $L_i^k = R_y(2\theta_k)$ is a rotation about \hat{y} axis by the angle θ_k and the corresponding constituent $C^{2n}(R_y(2\theta_k))$ in (4.12) is a generalized $2n$ -controlled rotation. From Corollary 1 and the fact that there are at most p generalized $2n$ -controlled rotations in (4.12), it follows that the complexity of \overline{R}_i is $O(pn)$ with the help of enough supporting qubits. This concludes the proof of the theorem.

Corollary 2 The time complexity of U_2 , given in (??), is $O(pn2^{2n})$ provided that enough supporting qubits are available in the working environment of U_2 .

Proof 4 The transformation U_2 is a composition of 2^{2n} transformation \overline{R}_i , and from Lemma 4, \overline{R}_i has complexity $O(pn)$ with the help of sufficient supporting qubits. Thus, the time complexity of U_2 is $O(pn2^{2n})$.

Theorem 2 The time complexity of preparation phase in IFRQI model is $O(pn2^{2n})$.

Proof 5 In IFRQI model, the complexity of Step1 in the preparation phase is $O(p+2n)$. And, from corollary 2, complexity of Step2 is $O(pn2^{2n})$. Thus, the time complexity of preparation phase in IFRQI model is $O(pn2^{2n})$.

4.2.2 IFRQI storage and its retrieval

The storage of IFRQI model is achieved by employing unitary transforms proposed in Sect. 4.2.1. On the other hand, the process of retrieving information from a given quantum state involves projective measurements. The projective measurements are performed on identical quantum states which results

in a probability distribution of all possible outcomes in the given set of basis vectors [15]. Each projective measurement has an associated self-adjoint operator, M , mapping state space (Hilbert space of all possible quantum states of the system under consideration) into itself. The measurement operator M has a decomposition $M = \sum_m P_m$. In it P_m is the projection operator and m are the eigenvalues.

The eigenvalues are the possible outcomes of projective measurements. The probability of getting output m in response of measuring the state $|\psi\rangle$ is $\langle\psi|P_m|\psi\rangle$. In the case where $\{|m\rangle\}$ form the computational basis of state space, the projector P_m is $|m\rangle\langle m|$, for each m . And, the result of application of measurement operator $M = \sum_m |m\rangle\langle m|$ on basis state $|\psi\rangle = |m\rangle$ is m with certainty. On the other hand, if $|\psi\rangle$ is not a basis state then projective measurements on identical copies of $|\psi\rangle$ yields a probability distribution. If we restrict the state space to only those quantum states ψ that are evolved under rotation gates $R_y(2\theta)$ ($0 \leq \theta \leq \frac{\pi}{2}$) as $|0\rangle \rightarrow R_y(2\theta)|0\rangle$, then, probability distributions associated to these states are distinct. Thus, the information about quantum state ψ can be retrieved from the information of probability distribution associated to it. Since FRQI model uses only single qubit to store the gray-scale information of each pixel in the image state and in the $2p$ -bit-deep images (normally value of p is 4), $2p$ classical bits are used for each pixel to represent its intensity, therefore, 2^{2p} different values, i.e., pixel's possible intensities, are encoded in amplitudes of a single qubit quantum state. This implies that there is a least difference in probability distributions, obtained through projective measurements on identical states, corresponding to pixels with small difference in their intensities. Thus, the accuracy of retrieving the information in FRQI model is low.

To enhance the retrievability of the image information, we encoded the classical 2-bit information in one qubit as shown in Table 4.2. Also, It is evident from the fourth and fifth column of Table 4.2 that there is a significant difference in probability distributions corresponding to quantum states in third column of Table 4.2. As described in Sect. 4.2.1, we use quantum state of p qubits to encode the gray-scale information of pixels with $2p$ -bits depth according to the rule given in Table 4.1. It follows that there is a significant difference in probability distributions of quantum states of p qubits obtained by unitary operations defined in Sect. 4.2.1. Thus, in IFRQI model, more accurate information can be retrieved from IFRQI state through projective measurements on few identical IFRQI states.

Table 4.2: Quantum states for the proposed encoding scheme and their probability distributions

Two bits information	Encoding angle θ	Quantum state	Probability of measuring	
			output 0	output 1
00	0	$ 0\rangle$	1	0
01	$\frac{\pi}{5}$	$\cos\frac{\pi}{5} 0\rangle + \sin\frac{\pi}{5} 1\rangle$	0.6545	0.3455
10	$\frac{\pi}{2} - \frac{\pi}{5}$	$\cos(\frac{3\pi}{10}) 0\rangle + \sin(\frac{3\pi}{10}) 1\rangle$	0.3455	0.6545
11	$\frac{\pi}{2}$	$ 1\rangle$	0	1

4.2.3 Image processing operations

In this subsection, we discuss the basic image processing operators for the proposed model. These operators can be divided into three groups in quite similar way to those presented in [15]. The three group are,

$$\begin{aligned}
\overline{G}_1 &= \otimes_{k=0}^{p-1} U_i \otimes I^{\otimes 2n} \\
\overline{G}_2 &= \otimes_{k=0}^{p-1} V_i \otimes C + I^{\otimes p} \otimes \overline{C} \\
\overline{G}_3 &= I^{\otimes p} \otimes W
\end{aligned} \tag{4.13}$$

where, U_i and V_i are single qubit matrices for each $i \in \{0, 1, 2, \dots, p-1\}$, W is $2n$ -qubit operator, I is the identity operator, C and \overline{C} are operators considering eligibility and ineligibility of positions, and $2n$ is the number of qubits encoding positions. The quantum circuits for these groups are presented in Fig. 4.5. The operators in group \overline{G}_1 has effect only on color qubits of IFRQI state, and the operators in group \overline{G}_2 has effect on color qubits against specified positions of IFRQI state, while, the operators in group \overline{G}_3 has effect on both color and position qubits of IFRQI state. Note that each operator in group \overline{G}_1 is a product of p single qubit operators, hence, its complexity is $O(p)$. The operator in \overline{G}_2 involves controlled rotations. Thus, complexity of operators in the group \overline{G}_2 is $O(N)$. The time complexity of operators in group \overline{G}_3 is $O(\log^2(N))$ [15].

Now, we illustrate the effects on IFRQI state corresponding to operators chosen from each of the above groups. The application of an operator in group \overline{G}_1 on the IFRQI state $|I_q\rangle$, transforms it into the quantum state as

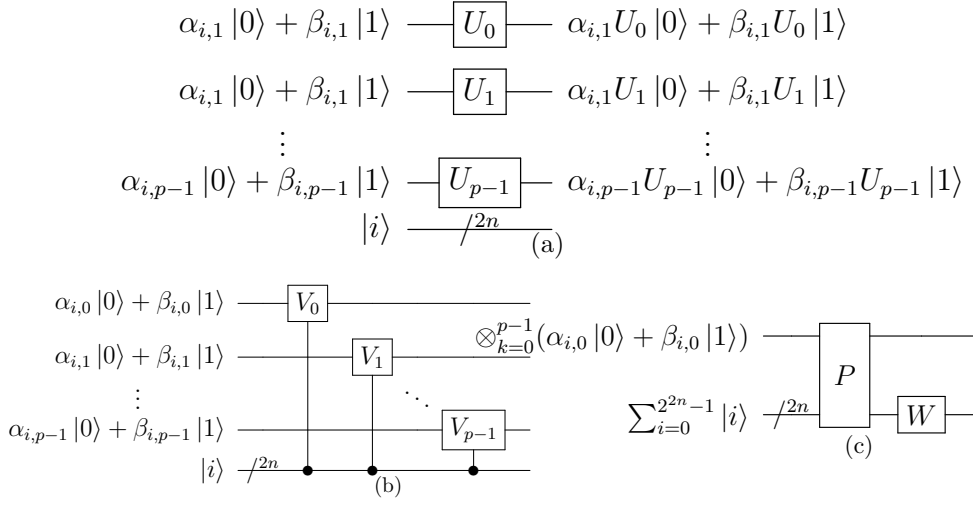


Figure 4.5: (a) Quantum circuit for \overline{G}_1 ; (b) Quantum circuit for \overline{G}_2 ; (c) Quantum circuit for \overline{G}_3

in (4.14).

$$\begin{aligned}
 \overline{G}_1|I_q\rangle &= (\otimes_{k=0}^{p-1} U_k \otimes I^{\otimes 2n}) \left(\frac{1}{2^n} \sum_{i=0}^{2^{2n}-1} (\otimes_{k=0}^{p-1} (\alpha_{i,k}|0\rangle + \beta_{i,k}|1\rangle)) \otimes |i\rangle \right) \\
 &= \left(\frac{1}{2^n} \sum_{i=0}^{2^{2n}-1} (\otimes_{k=0}^{p-1} (\alpha_{i,k} U_k |0\rangle + \beta_{i,k} U_k |1\rangle)) \right) \otimes |i\rangle \quad (4.14)
 \end{aligned}$$

In particular, if $U_k = X$ for each $k \in \{0, 1, \dots, p-1\}$, where $X = \begin{pmatrix} 0 & 1 \\ 1 & 0 \end{pmatrix}$, then (4.14) implies the quantum state (4.15).

$$\begin{aligned}
 \overline{G}_1|I_q\rangle &= (X^{\otimes p} \otimes I^{\otimes 2n}) \left(\frac{1}{2^n} \sum_{i=0}^{2^{2n}-1} (\otimes_{k=0}^{p-1} (\alpha_{i,k}|0\rangle + \beta_{i,k}|1\rangle)) \otimes |i\rangle \right) \\
 &= \left(\frac{1}{2^n} \sum_{i=0}^{2^{2n}-1} (\otimes_{k=0}^{p-1} (\beta_{i,k}|0\rangle + \alpha_{i,k}|1\rangle)) \right) \otimes |i\rangle \quad (4.15)
 \end{aligned}$$

The quantum state (4.15) is the IFRQI representation of the image, which is obtained by inverting all qubits in the color qubit sequence of $|I_q\rangle$. Furthermore, the operator $\overline{G}_1 = X \otimes I^{\otimes p-1} \otimes I^{\otimes 2n}$ transforms the IFRQI state $|I_q\rangle$ into (4.16), which represents the result image state obtained by inverting

two most significant bits of original image.

$$\begin{aligned}
\overline{G}_1|I_q\rangle &= (X \otimes I^{\otimes p-1+2n}) \left(\frac{1}{2^n} \sum_{i=0}^{2^{2n}-1} \left(\bigotimes_{k=0}^{p-1} (\alpha_{i,k}|0\rangle + \beta_{i,k}|1\rangle) \right) \otimes |i\rangle \right) \\
&= \left(\frac{1}{2^n} \sum_{i=0}^{2^{2n}-1} \left(\bigotimes_{k=0}^{p-1} (\alpha_{i,k}^0|0\rangle + \alpha_{i,k}^1|1\rangle) \right) \otimes |i\rangle \right) \quad (4.16)
\end{aligned}$$

where, $\alpha_{i,0}^0 = \beta_{i,0}$, $\alpha_{i,0}^1 = \alpha_{i,0}$, $\alpha_{i,k}^0 = \alpha_{i,k}$, $\alpha_{i,k}^1 = \beta_{i,k}$, for each $k > 0$ and $0 \leq i \leq 2^{2n} - 1$.

The operators in the group \overline{G}_2 change color value of pixels at specific positions, determined by the controlled matrix C . For instance, the operator (4.17) changes the color value of each pixel corresponding to first 2^{2n-1} positions in the IFRQI state $|I_q\rangle$ while the transformed state is given in (4.18).

$$\begin{aligned}
\overline{G}_2 &= \left(\bigotimes_{k=0}^{p-1} V_k \otimes \sum_{i=0}^{2^{2n-1}-1} |i\rangle\langle i| + I^{\otimes p} \otimes \sum_{i=2^{2n-1}}^{2^{2n}-1} |i\rangle\langle i| \right) \quad (4.17) \\
\overline{G}_2|I_q\rangle &= \left(\bigotimes_{k=0}^{p-1} V_k \otimes \sum_{i=0}^{2^{2n-1}-1} |i\rangle\langle i| + I^{\otimes p} \otimes \sum_{i=2^{2n-1}}^{2^{2n}-1} |i\rangle\langle i| \right) \\
&\quad \left(\frac{1}{2^n} \sum_{i=0}^{2^{2n}-1} \left(\bigotimes_{k=0}^{p-1} (\alpha_{i,k}|0\rangle + \beta_{i,k}|1\rangle) \right) \otimes |i\rangle \right) \\
&= \frac{1}{2^n} \left(\sum_{i=0}^{2^{2n-1}-1} \left(\bigotimes_{k=0}^{p-1} (\alpha_{i,k} V_k |0\rangle + \beta_{i,k} V_k |1\rangle) \right) \otimes |i\rangle \right) \\
&\quad + \sum_{i=2^{2n-1}}^{2^{2n}-1} \left(\bigotimes_{k=0}^{p-1} (\alpha_{i,k}|0\rangle + \beta_{i,k}|1\rangle) \right) \otimes |i\rangle \quad (4.18)
\end{aligned}$$

A special case of (4.17), with $V_k = X$ for each $k \in \{0, 1, \dots, p-1\}$, transforms the quantum image state $|I_q\rangle$ into the image state (4.19).

$$\begin{aligned}
\overline{G}_2|I_q\rangle &= \frac{1}{2^n} \left(\sum_{i=0}^{2^{2n-1}-1} \left(\bigotimes_{k=0}^{p-1} (\beta_{i,k}|0\rangle + \alpha_{i,k}|1\rangle) \right) \otimes |i\rangle \right) \\
&\quad + \sum_{i=2^{2n-1}}^{2^{2n}-1} \left(\bigotimes_{k=0}^{p-1} (\alpha_{i,k}|0\rangle + \beta_{i,k}|1\rangle) \right) \otimes |i\rangle \quad (4.19)
\end{aligned}$$

The quantum image state (4.19) is obtained by inverting every qubit, of color qubit sequence in $|I_q\rangle$, corresponding to first 2^{2n-1} positions.

The operators in the group \overline{G}_3 , change both color and position information. Since, each qubit of qubit sequence of color information involves $\alpha_{i,k} = \cos\theta_k$ and $\beta_{i,k} = \sin\theta_k$, therefore, the quantum Fourier transform (QFT) and quantum wavelet transform belongs to the group \overline{G}_3 . The application of QFT on IFRQI state is analogous to that of FRQI state [15]. The quantum state (4.20) represents the output image state obtained by the action of QFT on $|I_q\rangle$.

$$\begin{aligned} QFT(|I_q\rangle) &= \frac{1}{2^n} \left(\sum_{i=0}^{2^{2n-1}} \left(\bigotimes_{k=0}^{p-1} (\alpha_{i,k}|0\rangle + \beta_{i,k}|1\rangle) \right) \otimes QFT|i\rangle \right) \\ &= \frac{1}{2^n} \left[\sum_{m=0}^{2^{2n-1}} \left(\bigotimes_{k=0}^{p-1} (c_{m,k}|0\rangle + s_{m,k}|1\rangle) \right) \otimes |m\rangle \right] \end{aligned} \quad (4.20)$$

$$\begin{aligned} \text{where, } c_{m,k} &= \frac{1}{2^n} \left[\sum_{i=0}^{2^{2n-1}} e^{2\pi jim/2^{2n}} \alpha_{i,k} \right], \quad s_{m,k} = \frac{1}{2^n} \left[\sum_{i=0}^{2^{2n-1}} e^{2\pi jim/2^{2n}} \beta_{i,k} \right] \\ & \quad m = 0, 1, 2, \dots, 2^{2n} - 1. \end{aligned}$$

4.2.4 IFRQI compression

In classical image processing, image compression algorithms are used to minimize the number of resources required for construction of an image. In quantum image processing, the computational resources are quantum circuits used in the construction process of quantum image. It is a well-established approach to use minimization of boolean expression algorithms to decrease the complexity of quantum circuits, required for quantum image preparation.

As discussed earlier the time complexity of the first step of IFRQI preparation is $O(p+2n)$, which is already acceptable. And the second step of IFRQI preparation is the composition of 2^{2n} quantum operations \overline{R}_i , which can be decreased to simplify the quantum circuits. The complexity of preparation of quantum image is primarily based on the number of controlled rotations \overline{R}_i and its sub-operations $L_i^k = R_y(2\theta_k)$, which are applied on color qubits. Therefore, the main focus of this section is to reduce the number of controlled rotation gates required in the second step of image preparation.

The all requisite operation of second step are

$$\Phi = \bigcup_{i=0}^{2^{2n-1}} \bigcup_{k=0}^{p-1} \phi_i^k, \quad \phi_i^k = C^{2n}(R_y(2\theta_k)). \quad (4.21)$$

In Eq. (4.21), it is clear that p controlled rotations are used for every pixel in the image. To start with compression phase, the quantum operations given in (4.21) are divided into p groups expressed as in Eq. (4.22). Each group consists of all controlled rotations for the same qubit in the sequence of color qubits.

$$\Phi = \bigcup_{i=0}^{2^{2n}-1} \bigcup_{k=0}^{p-1} \phi_i^k = \bigcup_{k=0}^{p-1} \left(\bigcup_{i=0}^{2^{2n}-1} \phi_i^k \right) = \bigcup_{k=0}^{p-1} \Phi_k \quad (4.22)$$

Then each group is further categorised into 4 types of quantum sub operations. The category of quantum sub operation is determined by the value of $P_i^{2k+1}P_i^{2k}$ as mentioned in the Table 4.1, if $P_i^{2k+1}P_i^{2k} = 00$, angle θ_k is zero and the quantum sub operation becomes identity gate, which can be ignored. Therefore each group is mainly considered for 3 categories only as given in Eq. (4.23). Quantum operation in each category is a controlled rotation, which is controlled by a binary string. And then each category is compressed individually based on the value of rotation angle θ_k .

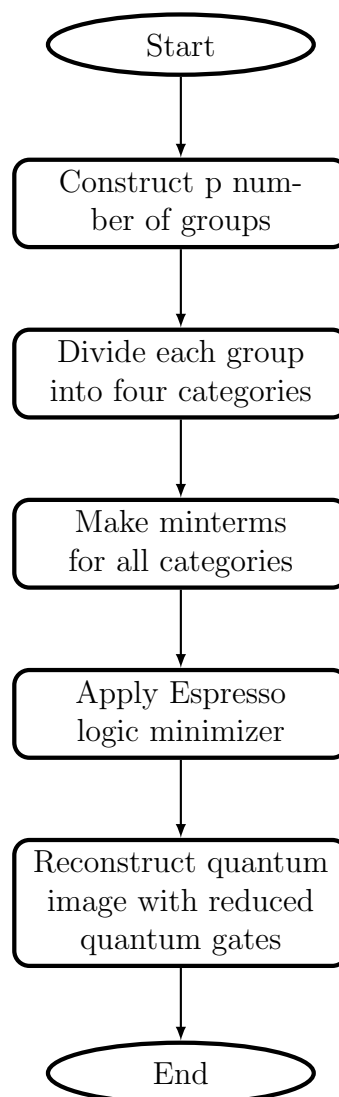
$$\begin{aligned} \Phi_k &= \bigcup_{i=0}^{2^{2n}-1} \phi_i^k \\ &= \left(\bigcup_{i=0, \theta_k=\pi/5}^{2^{2n}-1} L_i^k \right) \cup \left(\bigcup_{i=0, \theta_k=\pi/2-\pi/5}^{2^{2n}-1} L_i^k \right) \cup \left(\bigcup_{i=0, \theta_k=\pi/2}^{2^{2n}-1} L_i^k \right) \end{aligned} \quad (4.23)$$

where $L_i^k = C^{2n}(R_y(2\theta_k))$.

The next step is to transform the all positional information of each category to boolean minterms. We can make minterms simply by converting each position's binary string to a boolean variable, and then converting each Boolean variable to a minterm. Then Espresso logic minimizer takes controlled information, which are integration of all minterms as an input and produces reduced controlled information, which is then utilized to reconstruct reduced quantum circuits of a quantum image construction. Finally, after minimizing the boolean expression for each category, we can reconstruct the quantum image with fewer quantum gates. The step by step procedure of IFRQI compression is presented in Fig. 4.6.

The first step is to divide the IFRQI image into p groups, and each group is categorized in step 2. In third step, for each category boolean minterms are formed. Next step is to use logic minimizer to reduce the quantum gates and in the last step, reconstruct IFRQI image with fewer number of quantum operations.

Figure 4.6: Flow chart of the IFRQI compression procedure



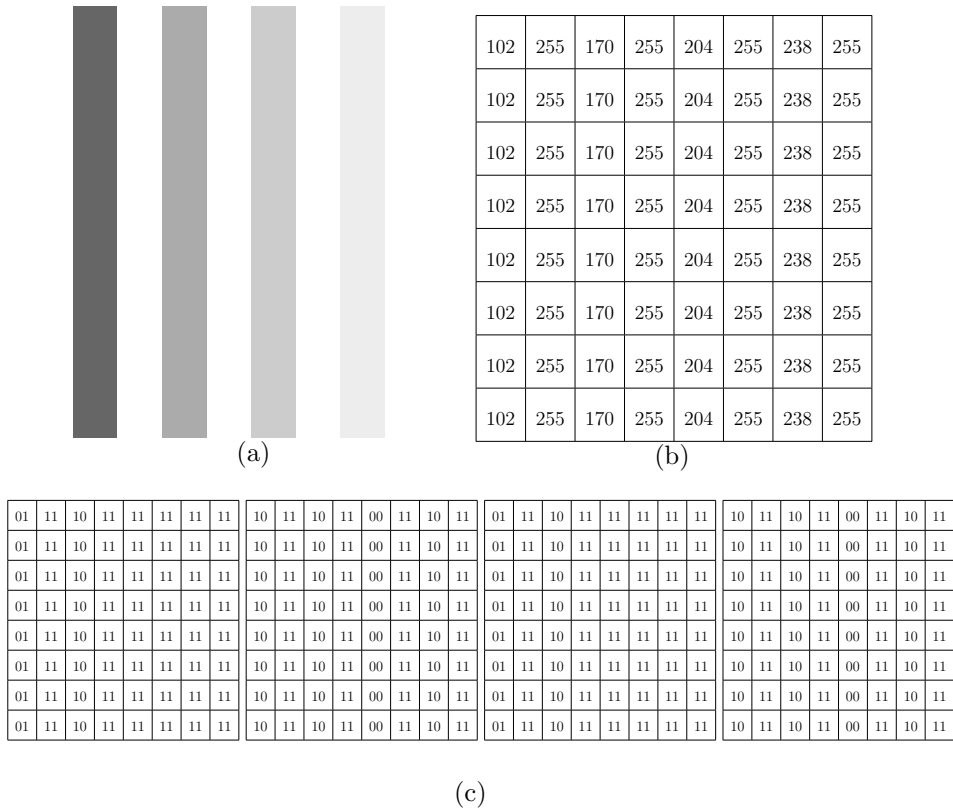


Figure 4.7: (a) an example of 8×8 image; (b) the gray-scale color value of pixel at each position; (c) p groups of quantum operation

We take the same image given in [33], for comparing the compression performance of NEQR and IFRQI. The image and its gray-scale values of all pixels are shown in Fig. 4.7. Figure 4.2.4 represents the 8×8 gray scale image with gray range of 256. Figure 4.2.4 shows the corresponding gray scale values of all pixels. If NEQR is used to construct the image, it would require 400 quantum gates before compression and 20 quantum gates after compression as mentioned in [33]. When IFRQI is used to store the same image it will require 240 quantum gates before compression and only 14 quantum gates after compression as shown below.

To illustrate the IFRQI compression procedure, we divide the image into p groups as shown in Figure 4.2.4, because gray range is 256, therefore the value of p is 4 in this example. Then we further divided each group into three categories 01, 10, 11 and then compressed each category individually. The reduced quantum operations for the four groups are represented as in .

The preparation of NEQR state of this image requires 400 quantum gates

Table 4.3: Reduced quantum operations for the four groups of Figure 4.2.4

		Group 1	Group 2	Group 3	Group 4
Category 1	Minimized expression	$x_0x_1x_2$	-	$x_0x_1x_2$	-
	Controlled rotation	$C^3(\pi/5)$	-	$C^3(\pi/5)$	-
Category 2	Minimized expression	$x_0x_1x_2$	$x_0x_1x_2, x_1x_2$	$x_0x_1x_2$	$x_0x_1x_2, x_1x_2$
	Controlled rotation	$C^3(\pi/2 - \pi/5)$	$C^3(\pi/2 - \pi/5), C^2(\pi/2 - \pi/5)$	$C^3(\pi/2 - \pi/5)$	$C^3(\pi/2 - \pi/5), C^2(\pi/2 - \pi/5)$
Category 3	Minimized expression	x_2 and x_0	x_2	x_2 and x_0	x_2
	Controlled rotation	$C^1(\pi/2), C^1(\pi/2)$	$C^1(\pi/2)$	$C^1(\pi/2), C^1(\pi/2)$	$C^1(\pi/2)$

before compression and 20 quantum gates after compression [33], whereas the preparation of IFRQI state of this image requires 240 quantum gates before compression and only 14 quantum gates after compression. To illustrate the IFRQI compression procedure for, we divide the image into p groups shown in Figure 4.2.4, because gray range is 256, therefore the value of p is 4. Then we further divided each group into three categories corresponding to 01, 10, 11, and then compressed each category individually. The reduced quantum operations for the four groups are represented as Table (4.2.4).

Following the procedure of IFRQI compression, the six example images presented in Fig. 4.8 are taken from [33]. To see the differences in compression performance of three image models, the number of gates before and after compression for each sample image is shown in Fig. 4.9. These results show that IFRQI is comparable with FRQI and NEQR.

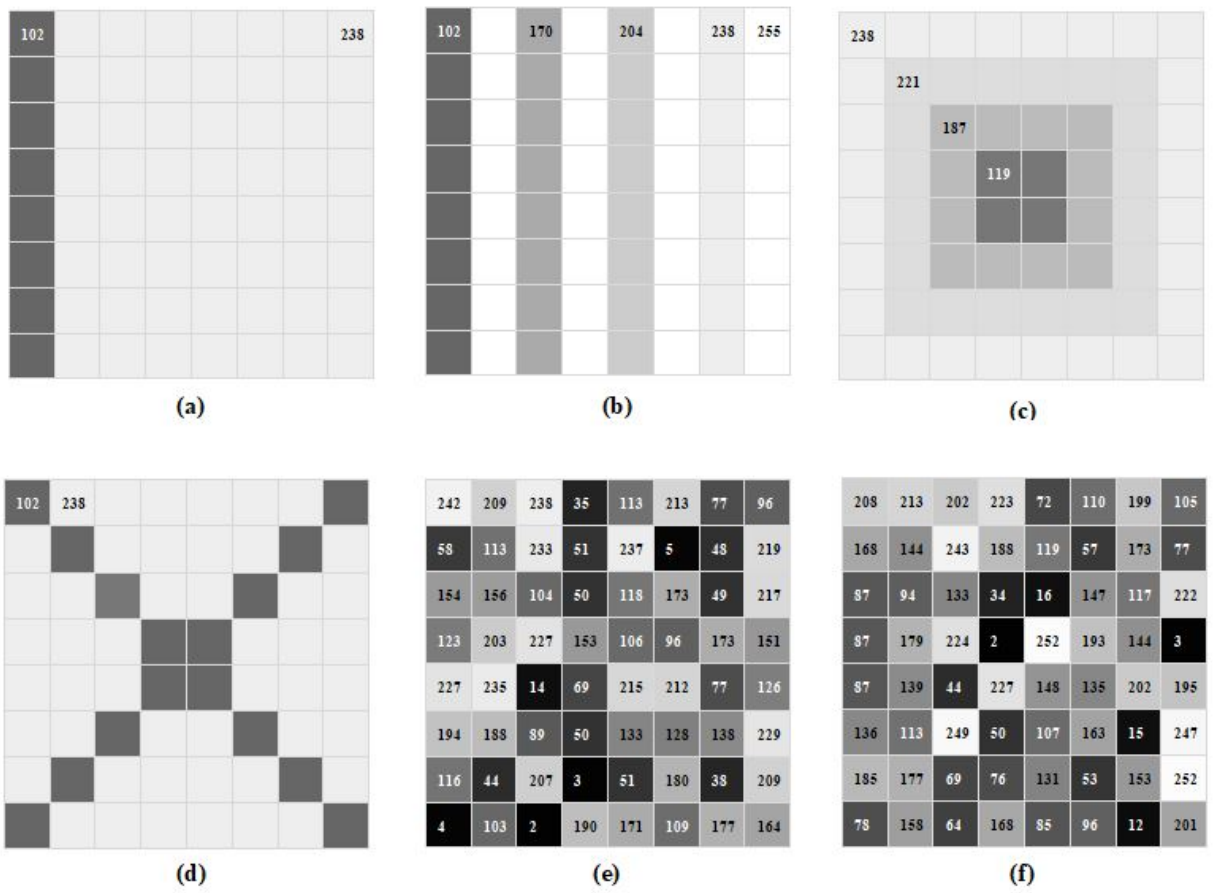
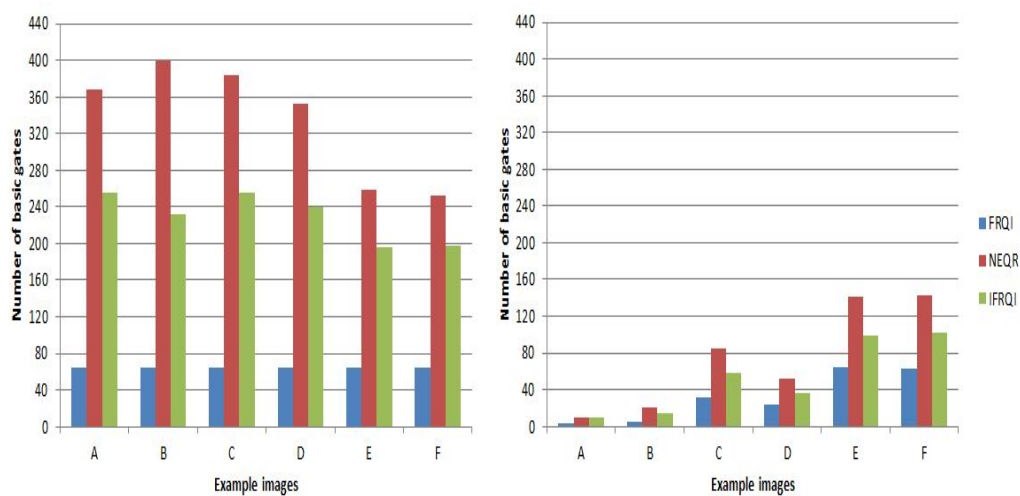


Figure 4.8: Example images with gray-scale distributions



(a) Before compression

(b) After compression

Figure 4.9: Comparison of number of gates used in quantum circuits of different image representation models

Chapter 5

Discussion, Conclusion and Future Directions

This chapter summarizes the main points of research that has been carried out in the thesis. And highlight the contributions of the proposed model in different fields of quantum image processing. The last section presents the potential future research work directions.

5.1 Discussion and conclusion

Section 4.1 shows that the complexity of image preparation in FRQI model is linear in the size of image. For an image of size $2^n \times 2^n$ with gray range 2^q , it is proved that the time complexity of FRQI model is $O(n2^{2n})$, whereas the complexity of NEQR model for the same image is $O(qn2^{2n})$. Thus, the time complexity of image preparation in FRQI model is lower than that in NEQR model. Also, by analyzing the FRQI and NEQR models, a new model IFRQI is proposed. The IFRQI uses two entangled qubit sequences to store color and position information of each pixel. An efficient method of encoding the classical 2-bit information in amplitudes of one qubit is given, which helps significantly in the accurate retrieval of original information from the probability distribution obtained through projective measurements. For an image of size $2^n \times 2^n$ with gray range 2^{2p} , it is established that the time complexity of image preparation phase of proposed model is $O(pn2^{2n})$, which is higher than that of FRQI but is comparable to NEQR. In addition, FRQI uses one qubit to store color information, and NEQR uses $2p$ qubits, whereas IFRQI uses p qubits. Accordingly, the space complexity issue is addressed in the proposed model with reference to the NEQR model. The quantum image processing operations for the proposed model are also discussed in detail.

The quantum image compression algorithm based on minimized boolean expression is presented and applied on example images. It is shown that the number of simple gates required, before compression and after compression, for IFRQI are comparable to those required for FRQI and NEQR.

5.2 Contributions

This research can contribute towards many fields such as quantum image steganography, quantum watermarking and quantum image encryption. Quantum image steganography is the practice of hiding secret information or message within some other non-secret carrier image. Hence the proposed model IFRQI can be used as a base framework for representing carrier image in quantum image steganography. Quantum water marking is the method of embedding owner's information into some carrier quantum image. And in quantum water marking technique, watermarked image can be represented in IFRQI form. Quantum image encryption is the art of transforming the meaningful image to meaning less image using some key. Therefore the IFRQI can provide a better way to represent quantum images for encryption strategies. Furthermore IFRQI can also be used in image scrambling techniques and grey codes.

5.3 Future research directions

This research provides many directions for future work in the world of quantum image processing. First of all the IFRQI model will be extended for storing, representing and processing color images. And some quantum image processing operators will be taken under considerations in detail, for future work. Furthermore, the research will be carried out to improve the compression algorithm of QIR models by exploring the different compression techniques.

Bibliography

- [1] Mona Abdolmaleky, Mosayeb Naseri, Josep Batle, Ahmed Farouk, and Li-Hua Gong. Red-green-blue multi-channel quantum representation of digital images. *Optik*, 128:121–132, 2017.
- [2] Adriano Barenco, Charles H Bennett, Richard Cleve, David P DiVincenzo, Norman Margolus, Peter Shor, Tycho Sleator, John A Smolin, and Harald Weinfurter. Elementary gates for quantum computation. *Physical review A*, 52(5):3457, 1995.
- [3] Glenn Beach, Chris Lomont, and Charles Cohen. Quantum image processing (quip). In *Applied Imagery Pattern Recognition Workshop, 2003. Proceedings. 32nd*, pages 39–44. IEEE, 2003.
- [4] Simona Caraiman and Vasile I Manta. New applications of quantum algorithms to computer graphics: the quantum random sample consensus algorithm. In *Proceedings of the 6th ACM conference on Computing frontiers*, pages 81–88. ACM, 2009.
- [5] David Deutsch. Quantum theory, the church–turing principle and the universal quantum computer. *Proc. R. Soc. Lond. A*, 400(1818):97–117, 1985.
- [6] Richard P Feynman. Simulating physics with computers. *International journal of theoretical physics*, 21(6):467–488, 1982.
- [7] Amir Fijany and Colin P Williams. Quantum wavelet transforms: Fast algorithms and complete circuits. In *Quantum Computing and Quantum Communications*, pages 10–33. Springer, 1999.
- [8] Lov K Grover. A fast quantum mechanical algorithm for database search. In *Proceedings of the twenty-eighth annual ACM symposium on Theory of computing*, pages 212–219. ACM, 1996.

- [9] shahrokh heidari and Ehsan farzadnia. A novel quantum lsb-based steganography method using the gray code for colored quantum images. *quantum information processing*, 16(10):242, 2017.
- [10] Shahrokh Heidari, Matin Vafaei, Monireh Houshmand, and Narges Tabatabaey-Mashadi. A dual quantum image scrambling method. *Quantum Information Processing*, 18(1):9, 2019.
- [11] Nan Jiang, Xuan Dong, Hao Hu, Zhuoxiao Ji, and Wenyin Zhang. Quantum image encryption based on henon mapping. *International Journal of Theoretical Physics*, pages 1–13, 2019.
- [12] Nan Jiang, Na Zhao, and Luo Wang. Lsb based quantum image steganography algorithm. *International Journal of Theoretical Physics*, pages 107–123, 2016.
- [13] Andreas Klappenecker and Martin Rotteler. Discrete cosine transforms on quantum computers. In *Image and Signal Processing and Analysis, 2001. ISPA 2001. Proceedings of the 2nd International Symposium on*, pages 464–468. IEEE, 2001.
- [14] Jose I Latorre. Image compression and entanglement. *arXiv preprint quant-ph/0510031*, 2005.
- [15] Phuc Q Le, Fangyan Dong, and Kaoru Hirota. A flexible representation of quantum images for polynomial preparation, image compression, and processing operations. *Quantum Information Processing*, 10(1):63–84, 2011.
- [16] Panchi Li and Ya Zhao. A simple encryption algorithm for quantum color image. *International Journal of Theoretical Physics*, 56(6):1961–1982, 2017.
- [17] Xiao-Zhen Li, Wei-Wei Chen, and Yun-Qian Wang. Quantum image compression-encryption scheme based on quantum discrete cosine transform. *International Journal of Theoretical Physics*, 57(9):2904–2919, 2018.
- [18] Hao-Ran Liang, Xiang-Yang Tao, and Nan-Run Zhou. Quantum image encryption based on generalized affine transform and logistic map. *Quantum Information Processing*, 15(7):2701–2724, 2016.
- [19] Michael A Nielsen and Isaac Chuang. Quantum computation and quantum information, 2002.

- [20] Qiwen Ran, Ling Wang, Jing Ma, Liying Tan, and Siyuan Yu. A quantum color image encryption scheme based on coupled hyper-chaotic lorenz system with three impulse injections. *Quantum Information Processing*, 17(8):188, 2018.
- [21] Jianzhi Sang, Shen Wang, and Qiong Li. A novel quantum representation of color digital images. *Quantum Information Processing*, 16(2):42, 2017.
- [22] H Shahrokh and N Mosayeb. A novel lsb based quantum watermarking. *Int. J. Theor. Phys*, 55(10):1–14, 2016.
- [23] Peter W Shor. Algorithms for quantum computation: Discrete logarithms and factoring. In *Foundations of Computer Science, 1994 Proceedings., 35th Annual Symposium on*, pages 124–134. IEEE, 1994.
- [24] Xian-Hua Song, Shen Wang, Shuai Liu, Ahmed A Abd El-Latif, and Xia-Mu Niu. A dynamic watermarking scheme for quantum images using quantum wavelet transform. *Quantum Information Processing*, 12(12):3689–3706, 2013.
- [25] Bo Sun, Abdullah M Iliyasa, Fei Yan, Fangyan Dong, and Kaoru Hirota. An rgb multi-channel representation for images on quantum computers. *Journal of Advanced Computational Intelligence and Intelligent Informatics*, 17(3):404–417, 2013.
- [26] Ru-Chao Tan, Tong Lei, Qing-Min Zhao, Li-Hua Gong, and Zhi-Hong Zhou. Quantum color image encryption algorithm based on a hyper-chaotic system and quantum fourier transform. *International Journal of Theoretical Physics*, 55(12):5368–5384, 2016.
- [27] Salvador E Venegas-Andraca and JL Ball. Processing images in entangled quantum systems. *Quantum Information Processing*, 9(1):1–11, 2010.
- [28] Salvador E Venegas-Andraca and Sougato Bose. Storing, processing, and retrieving an image using quantum mechanics. In *Quantum Information and Computation*, volume 5105, pages 137–148. International Society for Optics and Photonics, 2003.
- [29] Jian Wang, Ya-Cong Geng, Lei Han, and Ji-Qiang Liu. Quantum image encryption algorithm based on quantum key image. *International Journal of Theoretical Physics*, 58(1):308–322, 2019.

- [30] Leyuan Wang, Hongjun Song, and Ping Liu. A novel hybrid color image encryption algorithm using two complex chaotic systems. *Optics and Lasers in Engineering*, 77:118–125, 2016.
- [31] Ling Wang, Qiwen Ran, Jing Ma, Siyuan Yu, and Liying Tan. Qrci: A new quantum representation model of color digital images. *Optics Communications*, 438:147–158, 2019.
- [32] Wei-Wei Zhang, Fei Gao, Bin Liu, Heng-Yue Jia, Qiao-Yan Wen, and Hui Chen. A quantum watermark protocol. *International Journal of Theoretical Physics*, 52(2):504–513, 2013.
- [33] Yi Zhang, Kai Lu, Yinghui Gao, and Mo Wang. Neqr: a novel enhanced quantum representation of digital images. *Quantum information processing*, 12(8):2833–2860, 2013.
- [34] Yi Zhang, Kai Lu, Yinghui Gao, and Kai Xu. A novel quantum representation for log-polar images. *Quantum information processing*, 12(9):3103–3126, 2013.
- [35] Nan Run Zhou, Tian Xiang Hua, Li Hua Gong, Dong Ju Pei, and Qing Hong Liao. Quantum image encryption based on generalized arnold transform and double random-phase encoding. *Quantum Information Processing*, 14(4):1193–1213, 2015.
- [36] Nanrun Zhou, Yiqun Hu, Lihua Gong, and Guangyong Li. Quantum image encryption scheme with iterative generalized arnold transforms and quantum image cycle shift operations. *Quantum Information Processing*, 16(6):164, 2017.
- [37] Nanrun Zhou, Xingyu Yan, Haoran Liang, Xiangyang Tao, and Guangyong Li. Multi-image encryption scheme based on quantum 3d arnold transform and scaled zhongtang chaotic system. *Quantum Information Processing*, 17(12):338, 2018.
- [38] Ri-Gui Zhou, Ya-Juan Sun, and Ping Fan. Quantum image gray-code and bit-plane scrambling. *Quantum Information Processing*, 14(5):1717–1734, 2015.